

NAVAL POSTGRADUATE SCHOOL

Monterey, California



THESIS

**MOBILE SOURCE DEVELOPMENT FOR SEISMIC-SONAR BASED
LANDMINE DETECTION**

by

Douglas J. MacLean

June 2003

Thesis Advisor:
Second Reader:

Steven R. Baker
Thomas G. Muir

Approved for public release; distribution is unlimited

THIS PAGE INTENTIONALLY LEFT BLANK

REPORT DOCUMENTATION PAGE			<i>Form Approved OMB No. 0704-0188</i>	
Public reporting burden for this collection of information is estimated to average 1 hour per response, including the time for reviewing instruction, searching existing data sources, gathering and maintaining the data needed, and completing and reviewing the collection of information. Send comments regarding this burden estimate or any other aspect of this collection of information, including suggestions for reducing this burden, to Washington headquarters Services, Directorate for Information Operations and Reports, 1215 Jefferson Davis Highway, Suite 1204, Arlington, VA 22202-4302, and to the Office of Management and Budget, Paperwork Reduction Project (0704-0188) Washington DC 20503.				
1. AGENCY USE ONLY (Leave blank)		2. REPORT DATE June 2003	3. REPORT TYPE AND DATES COVERED Master's Thesis	
4. TITLE AND SUBTITLE: MOBILE SOURCE DEVELOPMENT FOR SEISMIC-SONAR BASED LANDMINE DETECTION			5. FUNDING NUMBERS	
6. AUTHOR(S) Douglas J. MacLean				
7. PERFORMING ORGANIZATION NAME(S) AND ADDRESS(ES) Naval Postgraduate School Monterey, CA 93943-5000			8. PERFORMING ORGANIZATION REPORT NUMBER	
9. SPONSORING /MONITORING AGENCY NAME(S) AND ADDRESS(ES) N/A			10. SPONSORING/MONITORING AGENCY REPORT NUMBER	
11. SUPPLEMENTARY NOTES The views expressed in this thesis are those of the author and do not reflect the official policy or position of the Department of Defense or the U.S. Government.				
12a. DISTRIBUTION / AVAILABILITY STATEMENT Approved for public release; distribution is unlimited			12b. DISTRIBUTION CODE	
13. ABSTRACT (maximum 200 words) <p>Landmines continue to be a threat to both military and civilian communities throughout the world. Current methods of detection, while better than nothing, could certainly be improved. Seismic SONAR is a promising new technology that may help save countless lives.</p> <p>The goal of this thesis was to advance Seismic SONAR development by introducing a mobile source which could be easily used in practical applications. A small tracked vehicle with dual inertial mass shakers mounted on top was used for a source. The source accurately transmitted the shaker signal into the ground, and its mobility made it a practical choice for field operations. It excited Rayleigh waves, as desired, but also generated undesirable P-waves and was not found to be directional. It proved incapable of finding a target.</p> <p>Improvements, such as a deploying an array of mobile sources and a stronger source, should vastly enhance the performance of such tracked vehicles in seismic SONAR mine detection and should be pursued.</p>				
14. SUBJECT TERMS Seismic SONAR, Landmine Detection, Seismic Waves			15. NUMBER OF PAGES 72	
			16. PRICE CODE	
17. SECURITY CLASSIFICATION OF REPORT Unclassified	18. SECURITY CLASSIFICATION OF THIS PAGE Unclassified	19. SECURITY CLASSIFICATION OF ABSTRACT Unclassified	20. LIMITATION OF ABSTRACT UL	

THIS PAGE INTENTIONALLY LEFT BLANK

Approved for public release; distribution is unlimited

**MOBILE SOURCE DEVELOPMENT FOR SEISMIC-SONAR BASED
LANDMINE DETECTION**

Douglas J. MacLean
Ensign, United States Navy
B.S., Cornell University, 2002

Submitted in partial fulfillment of the
requirements for the degree of

MASTER OF SCIENCE IN APPLIED PHYSICS

from the

**NAVAL POSTGRADUATE SCHOOL
June 2003**

Author:

Douglas J. MacLean

Approved by:

Steven R. Baker
Advisor

Thomas G. Muir
Co-Advisor

William B. Maier
Chairman, Department of Physics

THIS PAGE LEFT INTENTIONALLY BLANK

ABSTRACT

Landmines continue to be a threat to both military and civilian communities throughout the world. Current methods of detection, while better than nothing, could certainly be improved. Seismic SONAR is a promising new technology that may help save countless lives.

The goal of this thesis was to advance Seismic SONAR development by introducing a mobile source which could be easily used in practical applications. A small tracked vehicle with dual inertial mass shakers mounted on top was used for the mobile source. The source accurately transmitted the shaker signal into the ground, and its mobility made it a practical choice for field operations. It excited Rayleigh waves, as desired, but also generated undesirable P-waves and was not found to be directional. It proved incapable of finding a target.

Improvements, such as a deploying an array of mobile sources and a stronger source, should vastly enhance the performance of such tracked vehicles in seismic SONAR mine detection and should be pursued.

THIS PAGE LEFT INTENTIONALLY BLANK

TABLE OF CONTENTS

I.	INTRODUCTION.....	1
	A. MOTIVATION.....	1
	B. CURRENT METHODS OF MINE DETECTION.....	1
	C. OBJECTIVES.....	2
II.	SEISMIC WAVE PROPERTIES.....	5
	A. BODY WAVES.....	5
	1. Compressional Waves.....	5
	2. Shear Waves.....	6
	B. SURFACE WAVES.....	7
	1. Rayleigh Waves.....	7
	2. Love Waves.....	9
	C. SEISMIC WAVES FROM A VERTICAL SOURCE.....	10
III.	PRIOR RESEARCH.....	13
	A. UNIVERSITY OF TEXAS.....	13
	B. NAVAL POSTGRADUATE SCHOOL.....	13
	1. LT Stewart.....	13
	2. LT Gaghan.....	14
	3. LT Fitzpatrick.....	14
	4. MAJ Hall.....	14
	5. LT Sheetz.....	15
	6. LT McClelland.....	15
IV.	EQUIPMENT.....	17
	A. SOURCE DESIGN.....	17
	B. TRAILER.....	19
V.	TESTING.....	23
	A. TANK ROOM.....	23
	1. Source Choice.....	23
	2. Source Improvement.....	30

B. SOURCE PROPERTIES.....	32
1. Beam Pattern.....	32
2. Wave Classification.....	38
C. TARGET DETECTION.....	42
1. Detection with Oscilloscope.....	42
2. Detection with Human Ear.....	45
VI. CONCLUSIONS AND RECOMMENDATIONS.....	47
 APPENDIX A. MANUFACTURERS SPECIFICATIONS FOR AURA BASS SHAKER.....	 49
APPENDIX B. MANUFACTURER SPECIFICATIONS FOR GEOPHONE.....	51
APPENDIX C. MANUFACTURERS SPECIFICATIONS FOR ACCELEROMETERS.....	53
APPENDIX D. MATLAB CODE FOR "HILBRT.M".....	55
 LIST OF REFERENCES.....	 57
 INITIAL DISTRIBUTION LIST.....	 59

ACKNOWLEDGEMENTS

First, I would like to thank Professor Steve Baker for guidance and assistance in experimentation and the overall learning process, and LT Steve Rumph for assistance during experimentation. I would like to thank Professor Richard Harkins for allowing me to use his robotic tracked vehicle, “Bender”. Last, but not least, I would like to thank George Jaksha and Sam Barone for all of their electrical and mechanical assembly work, especially under tight time schedules.

THIS PAGE INTENTIONALLY LEFT BLANK

I. INTRODUCTION

A. MOTIVATION

Buried mines hinder operations for the US Armed Forces. Mines do so by three main methods: 1) inflicting casualties on soldiers, Marines, and sailors; 2) damaging or destroying equipment; and 3) changing battle plans due to the perceived threat of mines. They have proven to be an inexpensive, effective means of fighting for groups on the defensive. The threat of mines is especially relevant now due to the new role of the US Navy and Marine Corps, which is concentrated on going out and finding the enemy. Offensive forces which constantly push forward, like the US Armed Forces, provide the perfect target for land mines. 177 (13 percent) of the US casualties in the Gulf War of 1991 were due to Iraqi landmines and/or UXO (unexploded ordnance) (Stohl, 2002).

Mines also are a large problem for innocent civilians in countries which have hosted major conflicts over the last half century, such as France, Vietnam, Cambodia, Yugoslavia, Angola and Afghanistan. Annually, in Angola alone, there are approximately 6,000 new amputees due to landmines (VVAf, 1999). Worldwide, approximately 70 civilians are killed every day due to landmines that were left over from conflicts (Sheetz, 2000).

B. CURRENT METHODS OF MINE DETECTION

The most common method for finding land mines is to use a metal detector. This is both dangerous and slow. Metal detectors require the operator to be within 1-2m of the mine, which puts the operator within the “kill radius” of most landmines. Furthermore, metal detectors are inaccurate. They give a high number of false “hits” due to iron that may occur naturally in the ground. Also, they are useless against landmines made of something besides metal, such as plastic or vulcanized rubber.

Dogs can also be used to find mines, but they must be even closer to the mine than a metal detector. The obvious problem, from a strictly military viewpoint, is

inefficiency. Mine hunting dogs require time, money, and effort to train. It simply would not be worth it to invest that much in training a dog that will just get killed very soon after becoming operationally useful. They get tired and lose effectiveness after about an hour or two. Also, most trained sniffing dogs can only recognize one or two types of explosives, further limiting their usefulness.

Another technology under testing is commercially known as “Mongoose”. It consists of giant rope net grid (about half of a football-field size), with a small, shaped charge at each junction on the grid. This net is rocket-fired over a suspected minefield; it spreads out, and when it hits the ground, the shaped charges fire into the ground, detonating any landmines in the immediate surrounding area. While effective if shot at specific area known to have a high concentration of mines, it can also be very inefficient. Each shot is expensive, and more importantly, it does not find mines, it just detonates them if they are nearby. This could lead to a situation where dozens of nets are just shot all over the place, in hopes of finding mines, wasting money and time. If used in combination with a mine detection technology, the Mongoose system could be effective.

Ground penetrating RADAR (GPR) is another mine-detection technology under consideration. It is based on sending radio waves into the ground, and looking for returns, just like air based RADAR. However, GPR is very limited. Typical operating frequencies are around 300 MHz, which results in very short detection ranges due to high attenuation (Dolphin, 1997). Also, many soils are electrically conductive, which sharply decreases the range of GPR.

C. OBJECTIVES

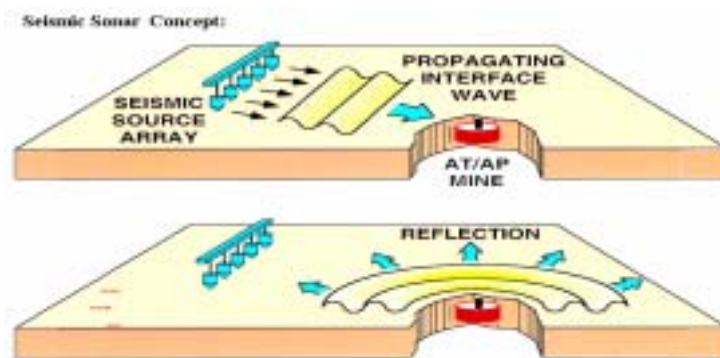


Figure 1. Seismic SONAR Concept

The concept of seismic SONAR is shown above. It consists of: sending energy into the ground, which propagates as seismic waves; and listening for an “echo” signal from the target.

The goal of this investigation was to develop and test a mobile source for a seismic SONAR mine detection system.

In meeting the goal, it was necessary to fulfill the following requirements:

- build or acquire a tracked vehicle that a vibration shaker system could be mounted on;
- test the rigidity of the vehicle to see if it was capable of transferring a clear signal to the ground;
- measure the received signal at various distances that could be transferred into the ground through the vehicle;
- establish a beam pattern;
- determine the types of waves which were propagating;
- find a target.

THIS PAGE LEFT INTENTIONALLY BLANK

II. SEISMIC WAVE PROPERTIES

Seismic waves travel through the ground. They place a strain on the ground, which acts as an elastic medium. The assumption that the ground acts elastically is valid because of the low level of ground deformation which occurs (Geophysics, St. Andrew's). In an earthquake, the first wave to arrive is the P-wave, or compressional wave. If there is a sub-surface reflection of the P-wave, then that reflection is next to arrive. After that, the s-wave, an elastic shear wave arrives. Last to arrive are the elastic surface waves (Seismo Lab, Cal Tech).

A. BODY WAVES

There are two types of body waves: compressional (P-waves); and shear (S-waves).

1. Compressional Waves

Compressional waves propagate longitudinally, i.e, the motion of the ground is in the same direction as the wave propagation. Particle motion is accordian-like, i.e., neighboring particles alternate between moving closer to each other and moving further apart. They are called “P-waves” because they arrive first (primary).

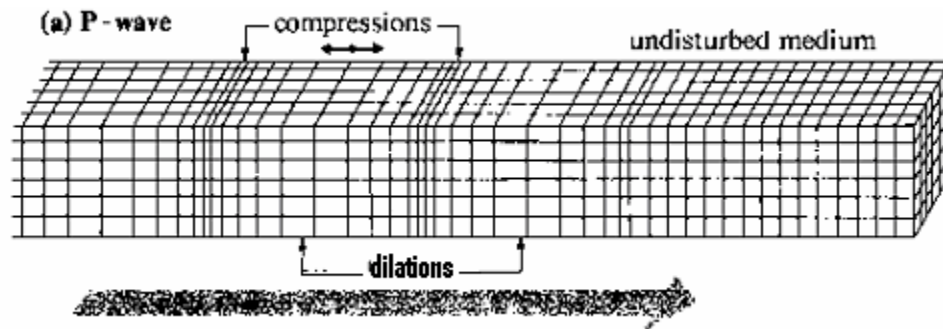


Figure 2. Propagation of a Compressional Wave (Brown et. al, 1981)

The compressional wave propagates with speed

$$V_p = \sqrt{\frac{k + 4\mu/3}{\rho}} \quad (2.1)$$

V_p is the speed, k is the bulk modulus of the ground, μ is the shear modulus of the ground, and ρ is the density of the ground.

P-waves are not desired in seismic mine detection because they are not confined near the surface of the ground, and can produce multiple, unwanted reflections from bottom layer boundaries which are deeper than the mine is buried. This results in many reflected rays arriving at sensors. These multiple, reflected ray paths make it difficult to differentiate between the initial drive signal, the bottom bounce reflection signals, and the return signal from the target. An illustration of bottom bounce is shown below in Figure 3.

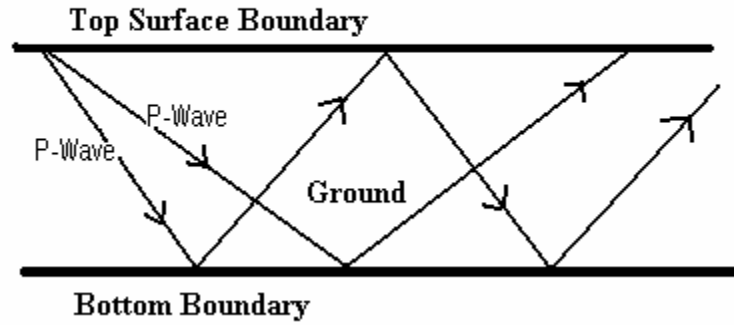


Figure 3. Bottom bounce reflection of a P-Wave.

2. Shear Waves

Shear waves propagate by shear strain, with the ground displacement perpendicular to the direction of propagation of the wave. They can be polarized either horizontally (SH) or vertically (SV). They are called “S-waves” because they arrive second, after the P-wave.

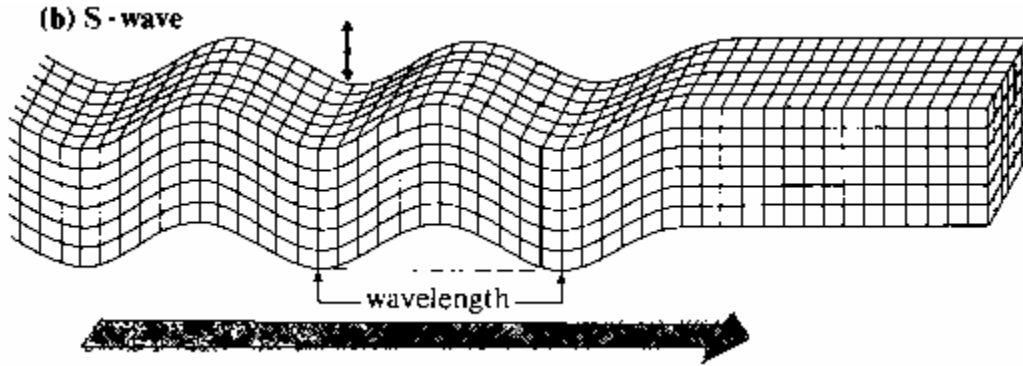


Figure 4. Propagation of a Shear Wave (Brown et. al, 1981)

The velocity of S-waves is:

$$V_s = \sqrt{\frac{\mu}{\rho}} \quad (2.2)$$

V_s is the velocity, μ is the shear modulus of the ground, and ρ is the mass density of the ground.

S-waves are also undesirable for mine detection because, like P-waves, they fill up the entire homogeneous half-space, and thus can produce multiple reflections.

Both types of body waves spread proportional to $1/r$ within the ground, where r is distance from the source. Along the surface, they spread proportional to $1/r^2$ (Gaghan, 1998).

B. SURFACE WAVES

1. Rayleigh Waves

Rayleigh waves travel relatively near the surface of the ground. The particle motion is in an elliptical orbit in a vertical plane perpendicular to the direction of wave propagation (Geophysics Dept., St. Andrews). The vertical and horizontal components of particle motion are 90° out of phase. Near the upper surface boundary (within 0.2 wavelengths), the motion is retrograde, i.e., the particles move counter-clockwise if the

wave is propagating from left to right (Fitzpatrick, 1998). This retrograde elliptical motion is shown by the darkened ellipse in Figure 5. At depths greater than 0.2 wavelengths, the particle motion switches to prograde, with the particles moving clockwise as the wave propagates left to right (Fitzpatrick, 1998), as shown in Figure 6.

Rayleigh Wave

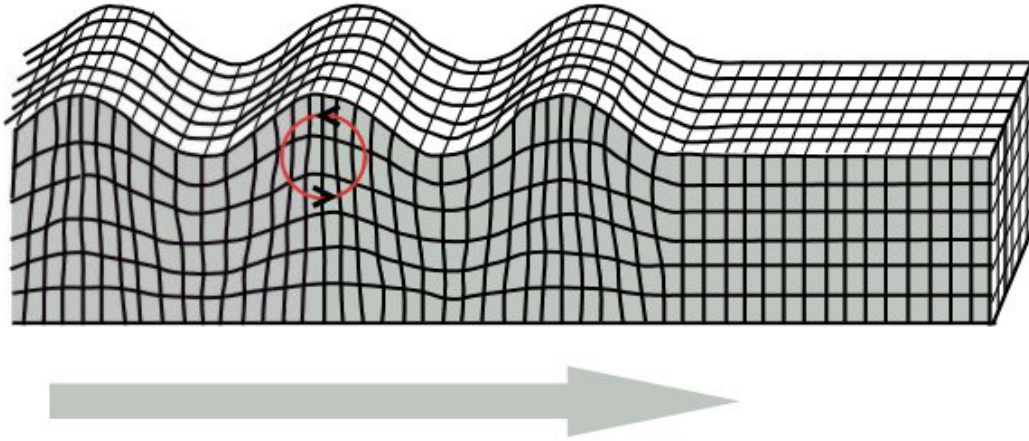


Figure 5. Propagation of a Rayleigh Wave (Brown, et. al, 1981)

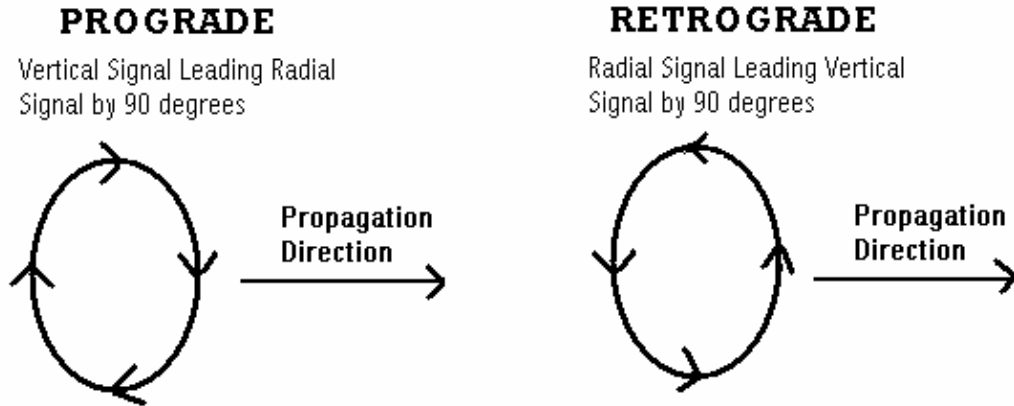


Figure 6. Prograde and Retrograde Rayleigh waves.

Rayleigh waves propagate with velocity:

$$c_r = c_s \kappa \quad (2.3)$$

where c_r is the Rayleigh wave speed, c_s is the shear wave speed, and κ is a dimensionless parameter, given by:

$$\kappa^6 - 8\kappa^4 + (24 - 16\gamma^2)\kappa^2 + (16\gamma^2 - 16) = 0$$

$$\gamma^2 = \frac{c_s}{c_l} = \frac{\mu}{\lambda + 2\mu} = \frac{1 - 2\nu}{2 - 2\nu} \quad (2.4 \text{ and } 2.5)$$

where γ is a dimensionless parameter, c_l is the longitudinal wavespeed, λ and μ are the Lamé constants, and ν is Poisson's Ratio (Fitzpatrick, 1998). For most solid/fluid boundaries (including sand/air) ν is approximately 0.25, and κ is approximately 0.9 (Fitzpatrick, 1998).

Rayleigh waves spread out with range proportional to $1/\sqrt{r}$. Recalling that body waves spread with $1/r$, over large horizontal distance, this difference in spreading rates results in Rayleigh waves being the dominant form of seismic energy. They also decay very rapidly with depth, carrying almost no energy deeper than 2 wavelengths (Seismo Lab, Cal Tech). This depth decay is ideal for seismic SONAR because it means that Rayleigh waves will not give strong reflections off of bedrock, etc., which would complicate the interpretation of return signals.

2. Love Waves

Love waves are ducted, horizontally-polarized shear waves. Their oscillations are in the plane of the surface of the ground, and perpendicular to the direction of propagation (see Figure 7). There was no interest with Love Waves for this project because they vibrate horizontally with respect to the ground. The source for this project vibrated vertically with respect to the ground, hence Love waves would only be minimally excited, if at all. However, they still could be used for mine detection with sources that vibrate horizontally with respect to the ground. Their main drawback is that they are a waveguide mode and possess multiple cutoff frequencies. They are also dispersive.

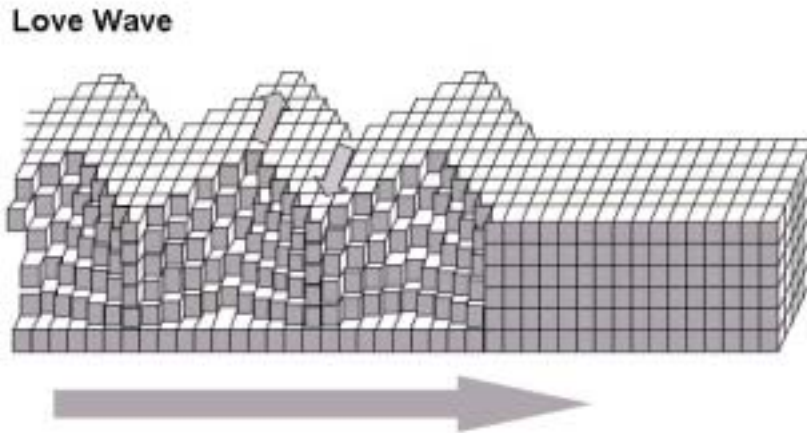
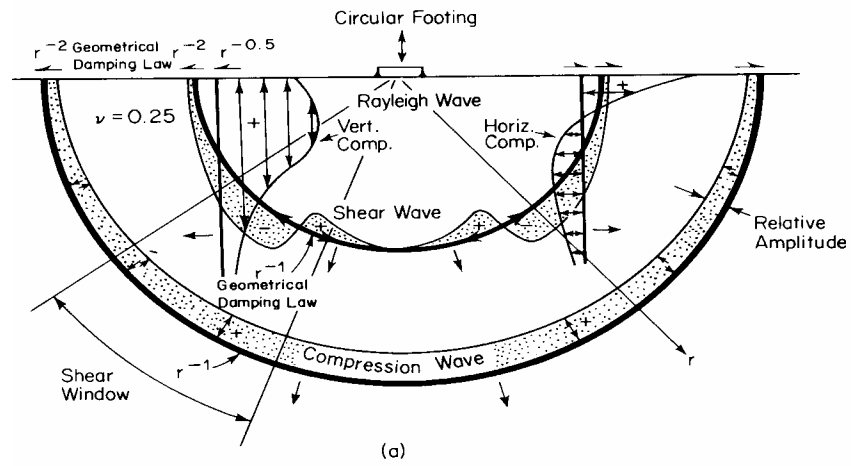


Figure 7. Love Wave Propagation, left to right (Brown, et. al, 1981)

C. SEISMIC WAVES FROM A VERTICAL SOURCE

Seismic wave interactions at a fluid-solid boundary depend on the boundary conditions (moduli, layering, etc.). These conditions determine the propagation speed, dispersion, depth of vibration in the sediment, and height of vibration in the air. For this research, the sand/air boundary resulted in negligible energy being transferred into the air. After a short settling distance, the resulting wave is a “smooth band” of seismic energy which propagates radially and vertically. This has been discussed in much greater detail in previous theses (Gaghan, Fitzpatrick, etc.)

Using geophones, it is possible to detect the ground disturbance caused by seismic waves. Seismic waves also scatter from strong enough inhomogeneties, such as a mine-like target, and can be detected. The ability to detect these waves is the basis for a seismic SONAR concept. As the figure below shows, ideally, the majority of energy that the geophones detect is in the form of Rayleigh waves. A major assumption of Fig. 8 below is that of a semi-infinite half-space, with no bottom interactions. If a bottom exists at a shallow enough depth where P-waves are still relatively strong, bottom bounce of P-waves could occur. Bottom bounce is when a wave bounces off the bottom, goes to the top surface, reflects off that, and continues this pattern of bottom/top reflection, moving horizontally all the while. A diagram of bottom bounce is shown above in Figure 3.



Wave Type	Per Cent of Total Energy
Rayleigh	67
Shear	26
Compression	7

Figure 8. Composite of all waveforms from a circular footing, in a homogeneous, isotropic, elastic half-space (Richart, et. al)

THIS PAGE LEFT INTENTIONALLY BLANK

III. PRIOR RESEARCH

A. UNIVERSITY OF TEXAS

Research on the seismic SONAR was initiated by Dr. Thomas Muir, then at the Applied Research Laboratories of the University of Texas at Austin (ARL:UT) in the 1990-1997 timeframe. This work was continued at NPS by Prof Muir when he assumed the chair professorship of Mine Warfare in the late 1990's. The research group's goal was to see if mines could be detected on a beach, for eventual applications to amphibious landings. The source used was a heavy rectangular plate with nails sticking out, and driven by an electro-mechanical transducer. They then set up seismometers and attempted to find a large metal cylinder.

While out in the field, they acquired echo ranging data for subsequent analysis. However, when they returned to their lab, they were able to detect the target after extensive signal processing. The signal processing included coherent averaging, background subtraction, and vector polarization filtering (Fitzpatrick, 1998).

B. NAVAL POSTGRADUATE SCHOOL

1. LT Stewart, USN

The first research at NPS was done by LT William Stewart in 1995 (Stewart, 1995). He created a conical-shaped plunger-type source using a loudspeaker mounted just above the ground, and tested its transmitted signal over a large range of frequencies. His testing was done in the large sand tank (an above ground swimming pool filled with sand) in the basement of Spanagel Hall. Using seismometers, he was able to show that his source could put a relatively strong seismic signal into the ground. However, the tank was too small for echo ranging experiments.

2. LT Gaghan, USN

Student Frederick Gaghan, with advisors Steven Baker and Thomas Muir, continued the research at NPS in 1998 (Gaghan, 1998). His focus was on source development and discrete-mode excitation.

His source consisted of two inertial mass shakers. He mounted them on an aluminum framework, so that each was pointing down at 45° . He had them at 45° because he needed two degrees of excitational freedom to excite elliptical Rayleigh waves. He was successful in preferentially exciting Rayleigh waves. He reported that discrete-mode excitation of Rayleigh waves had high potential, but a better source would improve the preferential Rayleigh excitation.

3. LT Fitzpatrick, USN

Student Sean Fitzpatrick, with advisors Steven Baker, Thomas Muir, and Anthony Healey picked up where LT Gaghan left off (Fitzpatrick, 1998). His focus was on improving source design from LT Gaghan's work. He ended up using a linear magnetic force actuator, which was also an inertial mass shaker, with a metal plate attached to a rod that pounded on the ground. He made the source water-tight so that it might have applications for mines buried in shallow water, such as the surf zone.

Using a two element seismometer array, he was able to locate 71 – 291 kg targets at ranges up to 5m.

4. MAJ Hall, USMC

Student Patrick Hall focused his research on target strength (Hall, 1998). He worked together with LT Fitzpatrick. He measured the reflectivity of targets as a function of their mass load. He found that target strength increased with increasing target mass.

5. CPT Sheetz, USA

Student Kraig Sheetz, with advisors Thomas Muir and Steven Baker, continued the seismic SONAR work at NPS in 2000 (Sheetz, 2000). He developed a new source and was able to locate an M-19, 20 lb, anti-tank mine. The source used was fourteen inertial mass shakers, mounted into seven pairs, laid out in a linear array and buried in the sand. The 7-element array provided high directionality, and he was able to focus a large amount of energy on the target. He was able to demonstrate signal to noise ratios of 9 dB in the echo from the anti-tank mine. While not the most practical of source designs, the size of a seven element array was good for detection, the concept of mine detection with seismic waves received a large boost of confidence.

6. LT McClelland, USN

Student Scott McClelland did work on rolling seismic SONAR source (McClelland, 2002). His source consisted of a two shaker mounted in a manually-pushed rolling cylinder. He was able to detect a 1000-lb bomb at 5 meters. The roller could only take readings when the shakers were directly aligned with the ground (i.e., once per cylinder revolution), and thus was not ideal.

THIS PAGE LEFT INTENTIONALLY BLANK

IV. EQUIPMENT

A. SOURCE DESIGN

It is essential for a deployable seismic SONAR system to have a mobile source. Simply stated, it is impractical to bring a system out into the field if it cannot be easily moved. With speed, adaptability, and efficiency being vital in today's battlefield, mobile source development is key in advancing the field of seismic SONAR.

Many ideas were considered, including: placing the source in a manually-pushed roller; placing the source on a sled, which could be pushed by an ATV; and placing the source on top of a tracked vehicle. After careful consideration of each, it was decided that mounting a source on top of a tracked vehicle would be the best. A tracked vehicle offered benefits such as: durability; and the ability to handle almost any terrain; compact size; and it could be remotely controlled, keeping operators away from mines.

Fortunately, a tracked vehicle was already available for use. This made the work considerably easier because construction of such a vehicle would have set us back several months. Professor Richard Harkins had obtained a remote controlled tracked vehicle for his robotics class, which he allowed us to use.

The robot was capable moving forward and backwards, turning left and right, and could be controlled remotely. However, all of the testing was performed with the robot stationary. The idea was that the robot could go to a location, send out seismic waves and look for mines, then move to another location and look for mines there. The robot is capable of sending out enough signals in a short period of time, to keep the speed and efficiency of mine detection high.

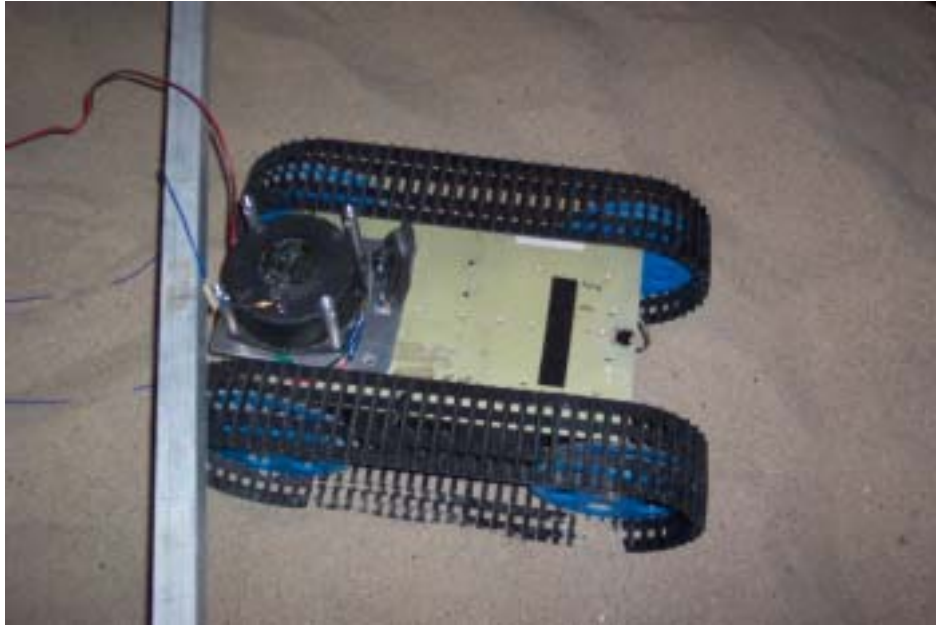


Figure 6. Robot with 1 shaker mounted.



Figure 8. Robot with 2 shakers mounted. The LCD screen is a digital compass. Upper right corner shows a 3-axis geophone.

The tracked vehicle used was 27 cm wide (cog to cog), 40 cm long, and 14 cm high (ground to top of chassis). Each cog was 16 cm in diameter. The robot mass was 12 kg when no equipment was mounted on it.

The robot moved by means of 4 fiberglass reinforced plastic, cogged wheels, with plastic tracks on each side. The body of the robot consisted of wiring, electronics, etc., with aluminum support rods, and outer aluminum plating to act as a shell.

A 1 cm thick, 14 cm x 14 cm square, aluminum plate was fastened to the top of the chassis of the robot, over the center of the front axle. Then, two Aura Bass Shakers (inertial mass shakers) were mounted on the plate, one shaker above the other. The bottom shaker was in direct contact with the plate, and the upper speaker was mounted on aluminum rods directly above the lower shaker. The shakers were wired in series, and so they “thumped” at the same time and in phase with each other. Each shaker was 1.2 kg, giving a total robot mass of 14.4 kg.

The shakers were centered on the axle because the axle was the most rigid part of the robot, and it also offered the most direct path of coupling between the source and the cogs. The theoretical assumption was that the robot source acts as a two-element array, with each front cog being one element of the array. In order to get a two-element array, the cogs and the source had to be coupled as well as possible. The rear axle of the robot was only confined to a slot, and held in place with springs. Therefore, it had some “play”. The front axle of the robot was fixed in place, and so the “play” was negligible compared to the rear. Also, by confining the signal to the front of the robot, it kept the footprint length down. At the chosen operating frequency, 100 Hz, the Rayleigh wavelength was about 1m. If the source was mounted in the center of the robot, the footprint would have been the length of the robot, or about half a wavelength. By limiting the signal transmission to the width of the robot (the front), the source was comparatively smaller in with respect to the produced wavelength (about one-quarter wavelength).

B. TRAILER

A trailer, designed and built by previous students working on seismic SONAR, housed all of the equipment. It was essentially a sheet-wood box on top of a metal trailer.



Figure 10. Equipment Trailer.

The headphone pre-amplifier was an RCA SA-155 Integrated Stereo Amplifier. The headphones were full ear cup Sony Noise-Canceling, model MDR-NC20. The headphones were used for listening to signals received by the geophones.

The geophones were tri-axial (x-, y-, and z-direction). This was achieved by having three single-axis geophones in a single housing. A representative drawing is shown below. Each geophone was potted in rubber and was waterproof. Jay Adeff constructed them.

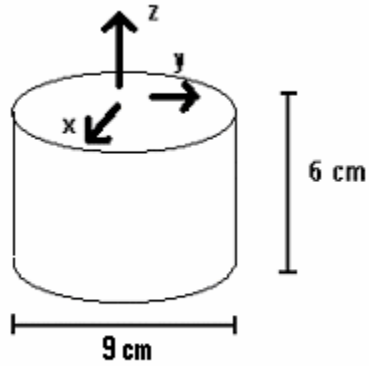


Figure 11. Drawing of a single geophone.

A calibration sheet is shown in Appendix B.

The Geophone Panel was designed by LT Stephen Rumph, and constructed by Samuel Barone. It was capable of receiving input from up to 18 geophones, with each geophone transmitting an x-, y-, and z-direction signal. The geophones could be grouped into 1 or 2 arrays. The panel was wired so that each geophone was in parallel with the other geophones. Output could be sent anywhere via BNC connection.

The power generator was gas powered and put out 2000 W. It was Honda, model 2000i.

The function generator created a drive signal for the transient burst measurements. It was a Hewlett Packard model 3314A.

The frequency filters were not used, as one did not even work and the other distorted the drive signal too much.

The drive signal amplifiers were used to amplify the signal out of the function generator. They were Carvin model DCM 1000, with 1000 W maximum output.

The oscilloscopes were used to view and store output from geophones and accelerometers. The majority of the transient burst measurements were done with a Tektronix TDS 3014 Four Channel Color Digital Phosphor Oscilloscope (pictured). For frequency scan response measurements, a Stanford Research Systems SR785 Signal Analyzer (not pictured) was used. For the target detection measurements, a Hewlett

Packard Infinium Two Channel Oscilloscope (not pictured) was used. It was used instead of the Tektronix because it had less internal electrical “noise”.

When on the beach, the trailer was towed with a John Deere “Trail Gator”. Typical cars were not capable of driving through the sand, so the “Gator” was necessary, and it performed well.

V. TESTING

Testing was conducted from February 2003 – May 2003. For all of February, and March, the testing was done in the sand-filled outdoor swimming pool located in Spanagel Hall Room 025. In April and May, testing was done: in the sand-filled tank; on the NPS softball field; and at Del Monte Beach.

A. TANK ROOM

1. Source Choice

The first task was to select a shaker. There were two options: a “Buttkicker 2”, made by The Guitammer Company; or dual “Bass Shakers”, wired in series, made by Aura (pictured in “Source Design” chapter).

For the purposes of testing the shakers, and for many subsequent tests, a transient burst signal was used. This signal was a single sine wave, at a given frequency and voltage, generated once per second. A qualitative representation of the drive signal used for testing is shown in Figure 12.

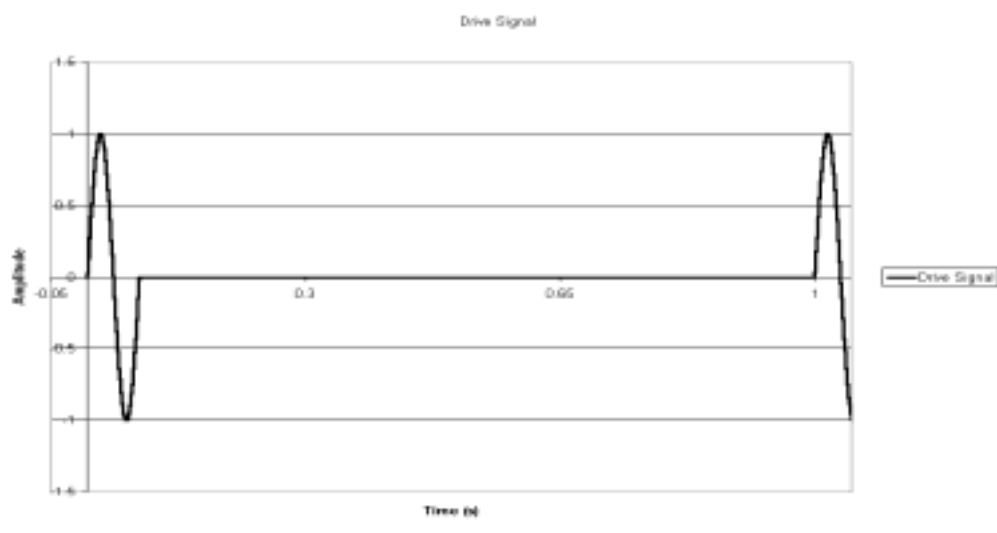


Figure 12. Representation of drive signal used in transient burst measurements.

As can be seen, there is a single sine wave burst at the beginning of each second.

The first source test was on the Buttkicker 2. The Buttkicker 2 is intended for the entertainment industry, to shake the floor in order to create the sensation of powerful bass in music. It is an electro-magnetic transducer that moves a 3.5 lb. inertial mass (a magnet) up and down. The mass is suspended magnetically, with no mechanical connections. It has a wide frequency range, from approximately 5 Hz to 200 Hz (Chiarealla, 2001).

Figure 13 shows the acceleration response of the robot for when a Buttkicker 2 was mounted on the on top of the chassis of the robot. Two PCB Piezotronics shear accelerometers, model J353B03, were used to record motion caused by the Buttkicker 2. Specifications for the accelerometers are shown in Appendix C. One accelerometer was mounted on the chassis directly above the front axle of the robot, and the other accelerometer was buried directly beneath the left front cog, approximately 3 inches deep. The Buttkicker was driven at 63.6 V (peak to peak) with a sine wave burst (one per second) at 100 Hz. The drive voltage was chosen so that acceleration would be approximately 1g. It was desired to keep robot chassis acceleration due to the shakers under 1 g so that the robot would not jump off the ground. Any jumping off the ground would cause non-linearities by sending an un-controlled wave into the ground, and would make signal processing more difficult. The same test was conducted at 50 Hz and 70 Hz, with similar results.

The y-axis shows acceleration response, in terms of [g], with $1g = 9.81m/s^2$, and the x-axis shows time in [s]. This plot is for a single sine wave drive burst. The averaging function of the Tektronix oscilloscope was used. Thirty-two averaging was chosen, which meant that the oscilloscope displayed an average of the last 32 signals it received, as opposed to showing each signal as it happened. The averaging function proved useful in clearing up random noise and interference. Thirty-two averaging was used on all testing involving using the Tektronix oscilloscope. The Tektronix was used

for measuring all transient burst measurements, unless otherwise noted. The response of the plate (black) is the signal with larger amplitude. The sand response is shown in gray.

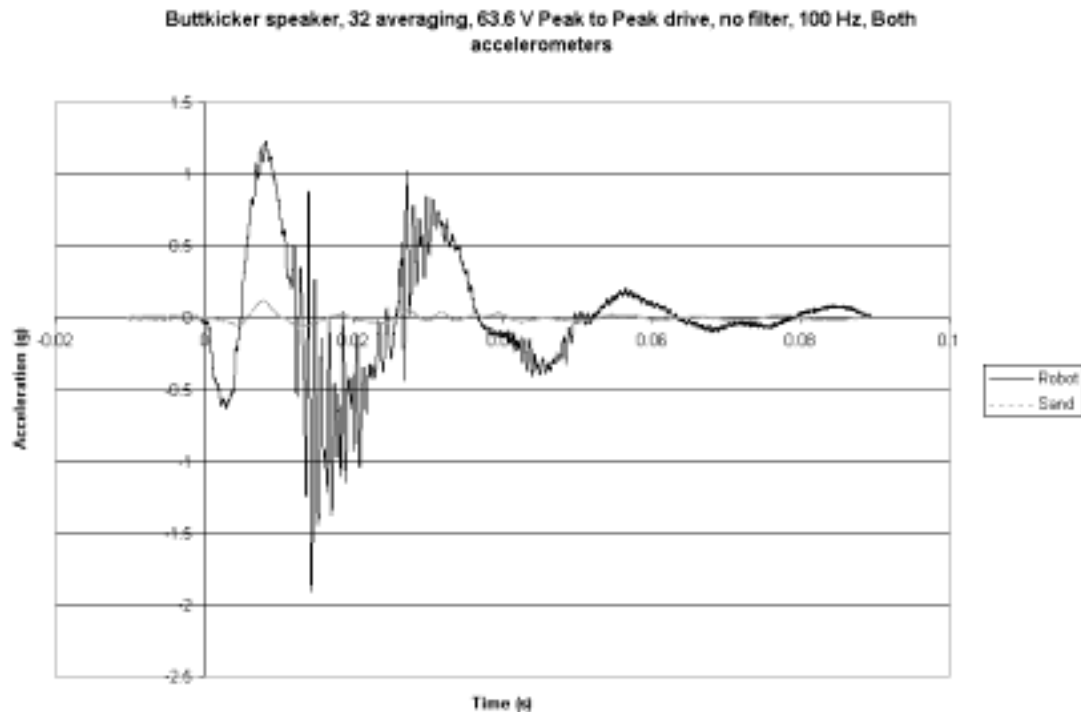


Figure 13. Robot and sand response with a ButtKicker 2 as a source.

Figure 13 shows that the ButtKicker 2 failed to deliver a “clean” signal. There was a lot of signal fluctuation on the robot around 0.02 seconds. These large signal fluctuations indicate non-linearities, which would complicate signal processing. Also, the signal from the ButtKicker 2 coupled poorly to the sand. There was approximately a 95% drop-off in acceleration amplitude. This plot indicates that the ButtKicker 2 is not a good source for testing, since the goal was a relatively clean, regular signal.

The other choice was the Aura Bass Shaker. Manufacturer’s specifications are in Appendix A. It is an electro-magnetic transducer. Similar to the ButtKicker 2, it moves a magnet up and down to generate vibration.

Figure 14 below shows information for the same experimental set-up as Figure 13 above, but dual Aura Bass Shakers were mounted on top of the chassis instead of a

Buttkicker 2. The drive signal was lower than for the Buttkicker 2 test (41.5 V peak to peak vs. 63.6 V), but acceleration was kept the same at approximately 1g. Robot acceleration response is shown in black, and sand acceleration response is in gray.

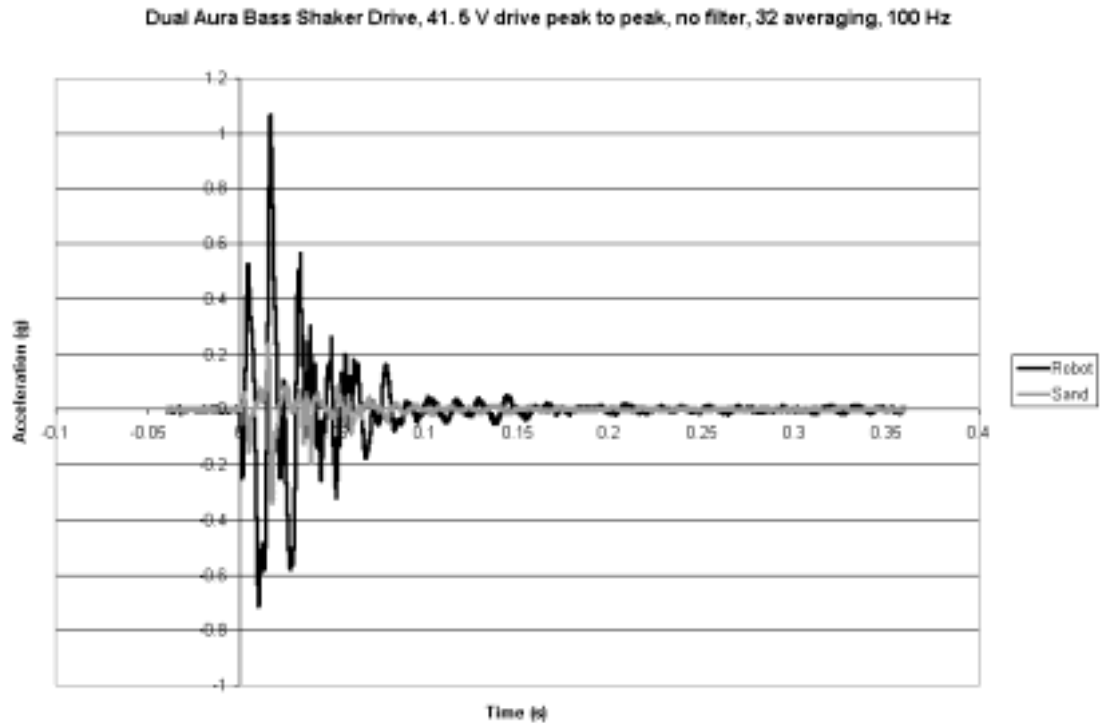


Figure 14. Robot and Sand acceleration response with dual Aura Bass Shakers as source.

The x-axis shows time in [s], and the y-axis shows acceleration response in [g]. As can be seen from the plot, the dual Aura Bass Shaker set-up delivered a much cleaner signal than the Buttkicker 2. There was no significant distortion anytime during the drive signal. Also, the signal transmission to the sand was stronger with Aura Bass Shakers. This plot shows approximately a 70% drop-off in acceleration amplitude from the robot to the sand, while the Buttkicker 2 showed approximately 95% drop-off. The gradual decrease in force amplitude over time in this plot indicates that there was some resonant ringing, which could not be avoided.

Before officially determining that Aura Bass Shakers would be used as the source, testing was done for further confirmation.

The first test involved seeing how much signal attenuation occurred in the robot itself with Aura Bass Shakers as source. This was accomplished by running two tests, both of which had one accelerometer mounted on top of the top shaker, and one accelerometer buried approximately 3 inches beneath the surface of the sand. The first test had the shakers mounted on the robot, and the second test had the shakers directly on the ground. On the “with-robot” experiment, the sand accelerometer was directly beneath the left front cog. On the “no-robot” experiment, the sand accelerometer was directly beneath the center of the shakers. The results are shown below.

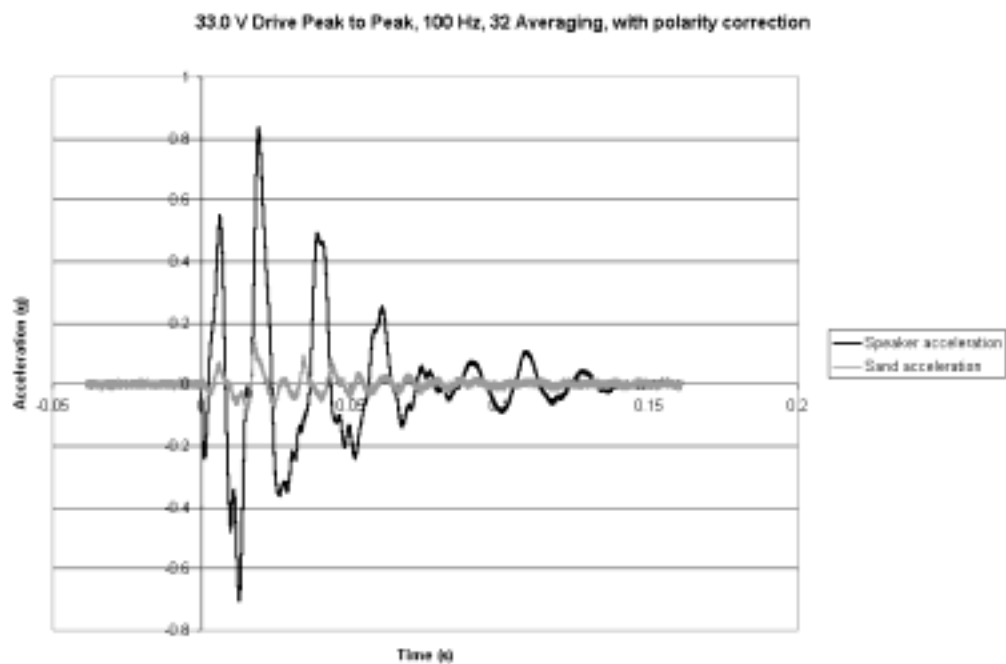


Figure 15. Sand and Shaker acceleration response when shaker mounted on robot.

Figure 15 shows the results for the shakers mounted on the robot. Time in [s] is shown on the x-axis, and acceleration response in [g] on the y-axis. Speaker acceleration response is in black, and sand acceleration response is in gray. Drive voltage was 33.0 V, peak to peak. Accurate transmission of phase and shape is shown, with a signal amplitude drop-off of approximately 85%. Resonant ringing was present.

Figure 16 shows force response curves for when the shakers were directly on the ground. These data are not shown on the same plot as the robot curve because it would be too much to show on one plot. The data would be unreadable.

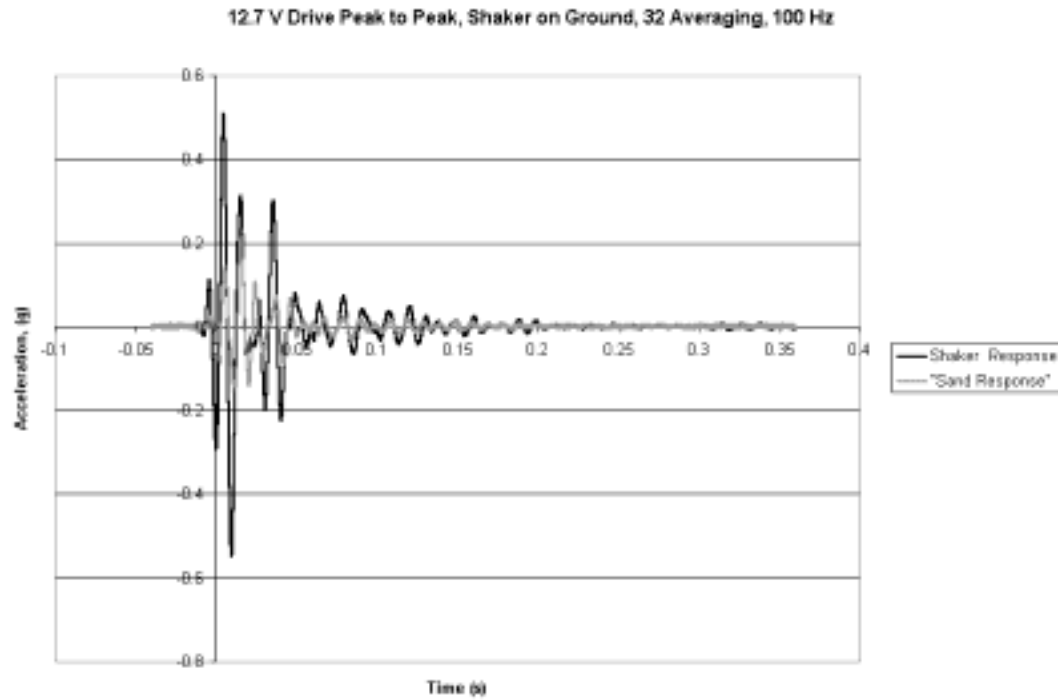


Figure 16. Shaker and Sand acceleration response for shaker mounted directly on ground.

This figure shows time in [s] on the x-axis and acceleration response in [g] on the y-axis. Acceleration response is shown in black, and sand acceleration response is shown in gray. Signal transmission was very good. Shape and phase were maintained, and the drop-off in acceleration amplitude was approximately 50%. There was some resonant ringing from the shaker case, but not as much as in the “with-robot” experiment.

Figure 17 shows a comparison of acceleration response of the robot vs. acceleration response of the shaker. Robot acceleration response is shown in gray, and shaker acceleration response is shown in black. The robot accelerometer was mounted on

the bottom of the front axle. Since it was mounted upside-down, a polarity correction had to be made, which was just multiplying the received signal by (-1) .

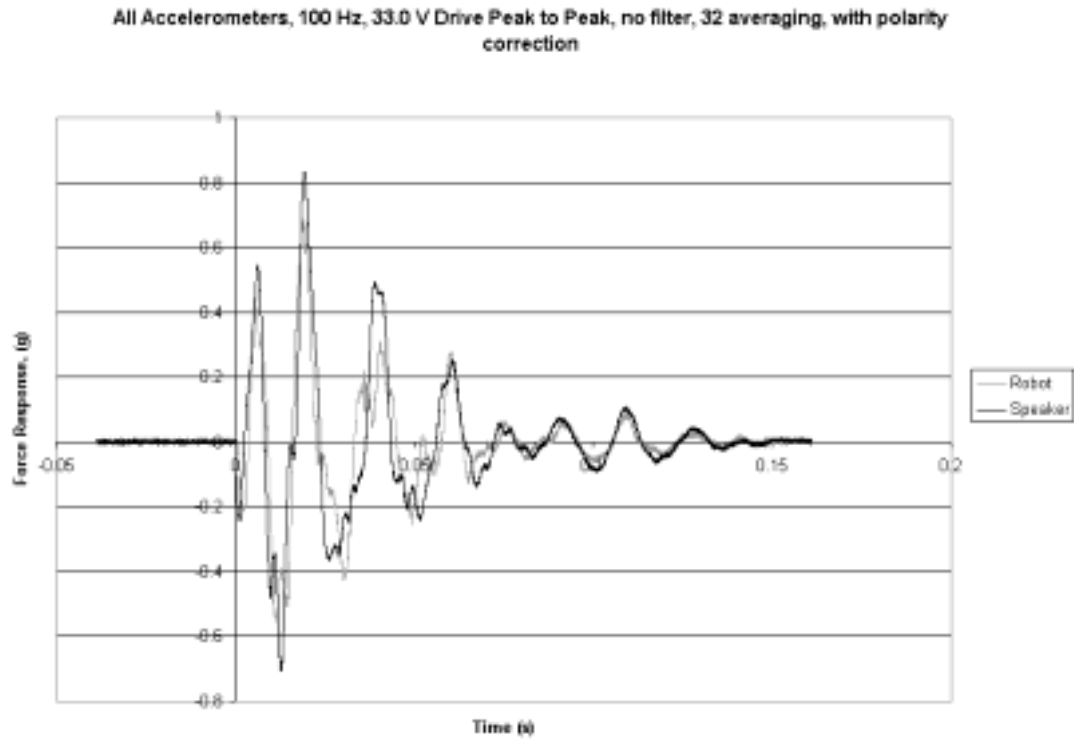


Figure 17. Shaker and robot force response curves.

Time in [s] is on the x-axis, and acceleration response in [g] is on the y-axis. Almost perfect signal transmission was shown through the body of the robot. Phase and shape were well maintained, with approximately a 15% drop-off in force amplitude. The same ringing was present as was present in previous experiments involving robot-mounted shakers.

These last three plots showed that the robot was responsible for both signal attenuation and some resonant ringing not present when the shakers were directly on the ground. The third plot showed almost perfect signal transmission from the shaker into the body of the robot, but the first plot showed significant decrease of the signal through the robot by the time it reached the sand. That indicated that the robot-caused losses occurred in between the body and the sand. The only objects in between the body of the

robot and the sand were the suspension springs, bearings, and the cogs. While the losses are unfortunate, they are unavoidable since suspension is needed for the robot to be an all-terrain vehicle.

2. Source Improvement

The Aura Bass Shakers showed a relatively clean, repeatable signal transmission into the sand, however there was significant power loss. One of the major requirements for landmine detection was a strong signal, so it was necessary to figure out a way to increase the signal strength. In response to this need, the dual Aura Bass Shaker set-up was kept, but added weight on top of to the chassis of the robot. After trying many different weights and arrangements, a lead brick laid on top of the chassis of the robot proved to work best. The brick was 18.5 kg, increasing total mass of the robot (robot, brick, and shakers) to 33.3 kg.

The robot accelerometer was mounted on the bottom of the front axle, and the sand accelerometer was buried 3 inches beneath the left front cog. Robot response is shown in black, and sand response is shown in gray.

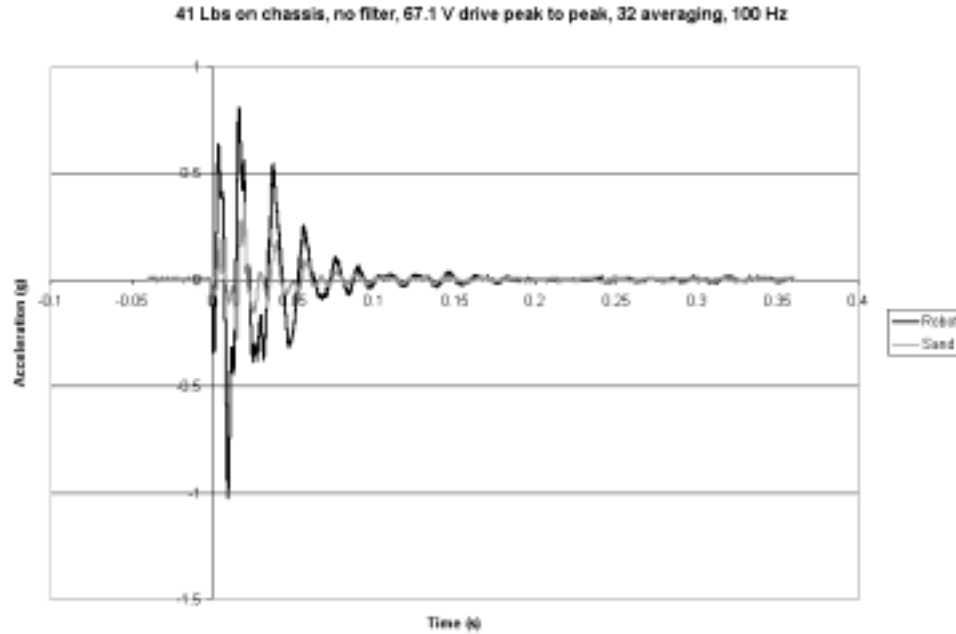


Figure 18. Robot and Sand force response for dual Aura Bass Shaker mount with weight added.

As Figure 18 clearly shows, there was a much improved signal transmission into the ground. Signal loss was reduced to approximately 50%, down from the 70% seen in Figure 15. A higher drive voltage was used than for an “un-weighted” robot, but robot acceleration was the same. The end result was that more force was put into the ground when a mass was laid on the chassis. In the “un-weighted” experiment, using $F=ma$, the shakers generated $1.05g \times 9.81m/s^2 / g * 13.4kg = \underline{138N}$ of force. In the “with-weight” experiment, the shakers generated $.80g \times 9.81m/s^2 / g \times 33.3kg = \underline{261N}$ of force. If the acceleration was taken up to 1g, as in the un-weighted experiment, 326 N could have been generated. Clearly, placing weight on the chassis increased force generation and improved the quality of the source.

Despite the amplitude loss and resonant ringing, the quality of signal transferred into the ground was still clean and repeatable, and thus further experimentation with the robot-mounted source was worthwhile. Dual Aura Bass shakers were acceptable.

B. SOURCE PROPERTIES

1. Beam Pattern

The first task in determining source properties was directionality. It was assumed the robot would act as a two-element array, with each front cog acting as one element. In order to test this assumption, testing was done at the NPS softball field. The trailer was set up in foul territory near third base, and the robot was on the infield near second base, approximately 25 meters away from the trailer. The infield was made of packed dirt. One geophone was placed 2m away from the robot, and another geophone was 4m away (shown below). The geophones were placed on the surface of the ground.



Figure 19. Photo of testing set-up on softball field.

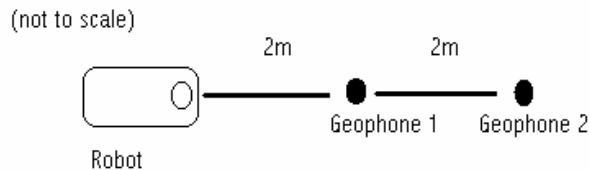


Figure 20. Schematic of testing on softball field.

Ground truthing (sound speed measurements) were the first test performed. A single impulse was generated by the shakers, and each geophone received the signal. The time delay between when each geophone received a signal from the robot was recorded. The distance between the geophones was set at 2m. It was then possible to calculate speed of sound with the time it took for the signal to get from the first geophone to the second. The speed was calculated at 170 m/s.

The robot was kept stationary, and the geophones were rotated around it. Readings were taken every 30°. Measured beam pattern was calculated by the following means: the maximum received voltage at each bearing was noted and squared; the squared voltage from each angle was then plugged into

$$BeamPattern(\theta) = 10 \times \log_{10} [signal(\theta) / signal(0^\circ)]. \quad (5.1)$$

This beam pattern was then compared to a theoretical beam pattern. As stated above, the robot was modeled as a two-element array with N=2 (number of elements). Spacing between elements was d=0.27m. The wave number “k” was calculated using:

$$k = 2\pi f / c \quad (5.2)$$

Where f = frequency, and c = speed of sound. The directional factor, H, was calculated using:

$$H(\theta) = \left| \frac{1}{N} \frac{\sin[(N/2)kd \sin \theta]}{\sin[(1/2)kd \sin \theta]} \right| \quad (\text{KFCS, 2000}) \quad (5.3)$$

Where N = number of elements, k = wavenumber, d = spacing between elements, and θ = bearing of geophones relative to the front of the robot. Theoretical beam pattern was then calculated using:

$$BeamPattern(\theta) = 20 \times \log_{10} (H(\theta)) \quad (\text{KFCS, 2000}). \quad (5.4)$$

The results are shown in Figure 21. Measured beam pattern is in black, and theoretical beam pattern is in gray. The numbers around the outside of the plot indicate geophone bearing relative to the robot in [deg], and the magnitude scale is in [dB].

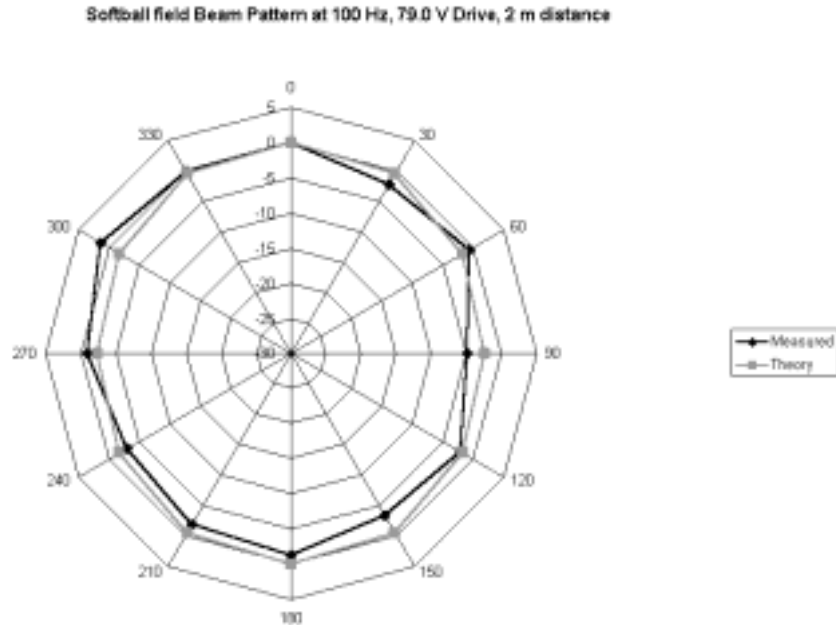


Figure 21. Measured vs. Theoretical beam pattern at the softball field.

The theoretical and measured beam patterns match up well enough to not disprove that the two-element assumption was correct. At the softball field, a 100 Hz single cycle tone burst was the only signal used. Tests using different signals would be performed later at Del Monte Beach.

It was desired to know if the source had the same properties in different media, so further beam pattern testing was performed at Del Monte Beach. The testing was done according to the same protocol as at the softball field. Ground truthing was also performed. An example is shown below. A lead brick was dropped, and each geophone picked up the signal. As explained above, the time between received signals was divided by distance between the geophones. An example plot of data from ground truthing is shown in Figure 22. The response of the near geophone is shown in black, and the response of the far geophone is shown in gray.

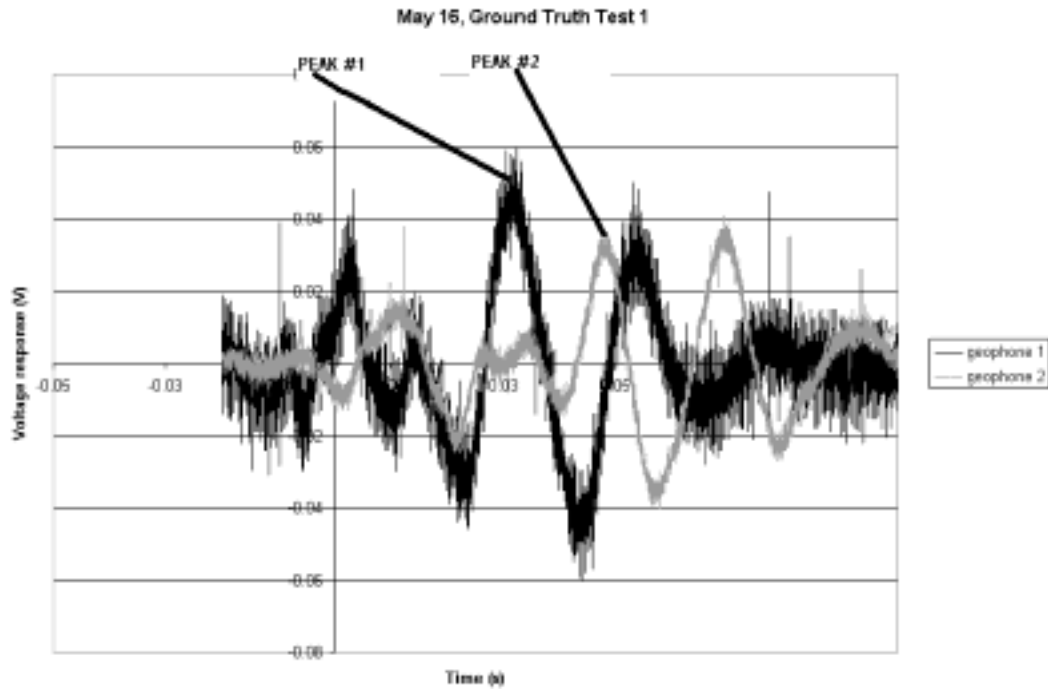


Figure 22. Ground truth example.

The time between peaks was 0.0166 seconds. Given a 2m distance between geophones, the speed of sound in the ground was 120m/s. Further trials confirmed that speed.

Beam patterns were also calculated the same way at the beach as at the softball field. Figure 23 shows the beam pattern for a single –cycle tone burst at 100 Hz. The geophones were partially buried.

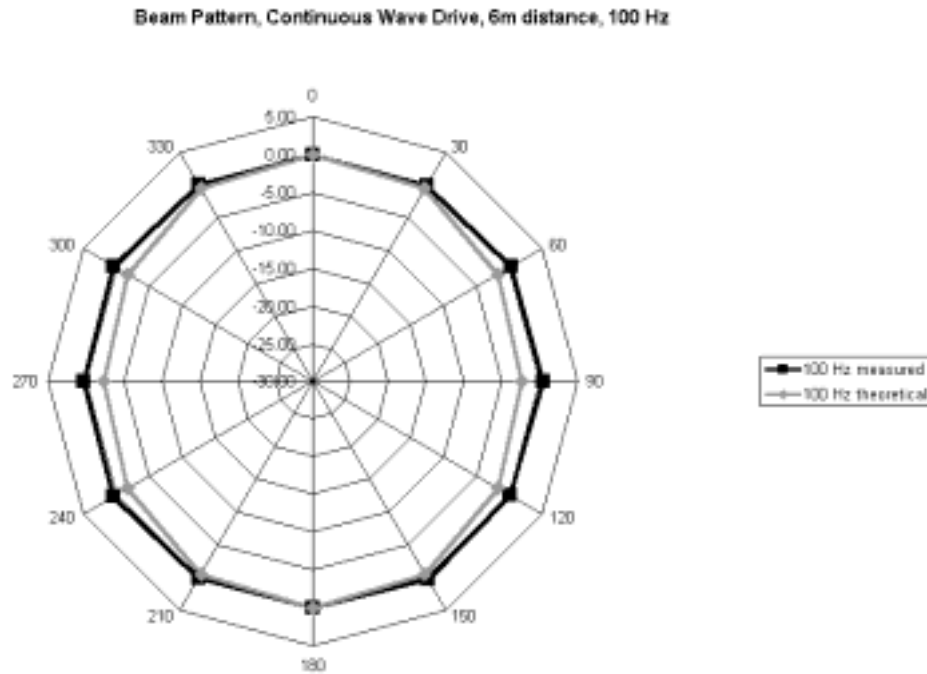


Figure 23. Beam pattern at the beach, 100 Hz, 6m distance.

Theory and measured matched up almost exactly. With that, it was seen that the robot acted as an omni-directional source. Further testing involved increasing the drive frequency. This was done to see if the robot could be estimated as a two-element array. Figure 24 shows the beam pattern for a single-cycle tone burst at 200 Hz. Measured is in black, and theoretical is in gray.

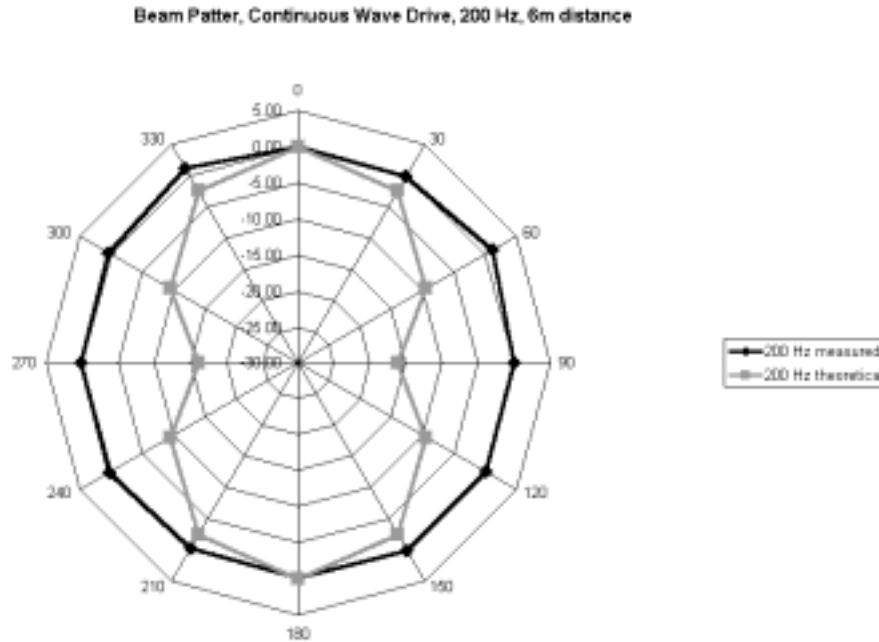


Figure 24. Beach beam pattern at 200 Hz, 6m distance.

Geophone bearing in [deg] relative to the robot is shown by the numbers outside the graph, and beam pattern in [dB] is shown on the magnitude scale. As can be seen, the measured beam pattern does not match up to the theoretical beam pattern. The disparity between measured and theoretical grew even larger as frequency was increased to 200 Hz and 250 Hz. There were two possible conclusions from this: a) the tone burst had mixed P-waves and Rayleigh waves at this distance, and tests should be repeated at a greater range which would allow the wave types to separate; or b) the robot could not be approximated as a two-element array and displayed no directionality as a source. This second conclusion would be most unfortunate, as directionality would allow beam-steering. Beam steering would greatly increase the accuracy of mine hunting because the operator could get a mine bearing as well as distance.

2. Wave Classification

The next task was to determine which type of waves propagated from the robot. This was done using the Stanford Research Systems SR785 Signal Analyzer. Measurements were taken using a continuous wave frequency scan. This meant that the SR785 put out a continuous wave that started at a low frequency (ex. 50 Hz) and ended at a higher frequency (ex. 250 Hz). The frequency scan took approximately 30 seconds to complete. Voltage response of the geophones was recorded at each frequency. The SR785 was capable of recording signal magnitude and phase.

After doing ground truthing, the sound speed of the day was found to be 100 m/s. It was necessary to make approximations. Referencing equation (2.5), Poisson's ratio for sand is typically $\nu = 0.25$ (Fitzpatrick, 1998). This gives a ratio of shear wave speed to longitudinal speed, $\gamma^2 = 0.429$. Then, solving by iteration, it was found that the ratio of Rayleigh wave speed to the shear wave speed, $\kappa = 0.898$. This then indicated a Rayleigh wave speed of $0.898 \times 100 \text{ m/s} = 90 \text{ m/s} = c_r$. For a Poisson's Ratio of $\nu = 0.25$, the P-Wave speed is approximately 3 times the Rayleigh wave speed (Gaghan, 1998). That led to a P-Wave speed of 270 m/s.

The next experiment was to determine if Rayleigh waves were excited. To do this, radial and vertical phases were recorded as a function of frequency, while doing a frequency scan with the SR785. Both the radial and vertical components were measured by the same geophone. The set up for the phase difference experiment is shown in Figure 25.

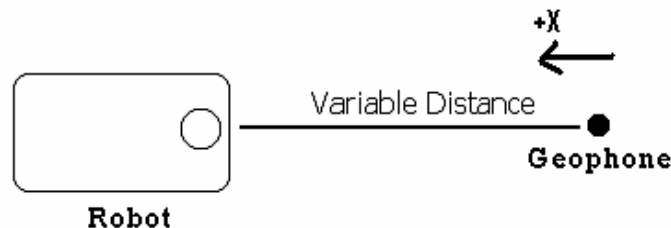


Figure 25. Set up for phase difference measurements.

Figures 26 a) and b) show phase difference, radial component minus vertical component, of the signal put out by the robot. The geophone was oriented so that radial geophone motion towards the robot was recorded as positive radial phase measurement.

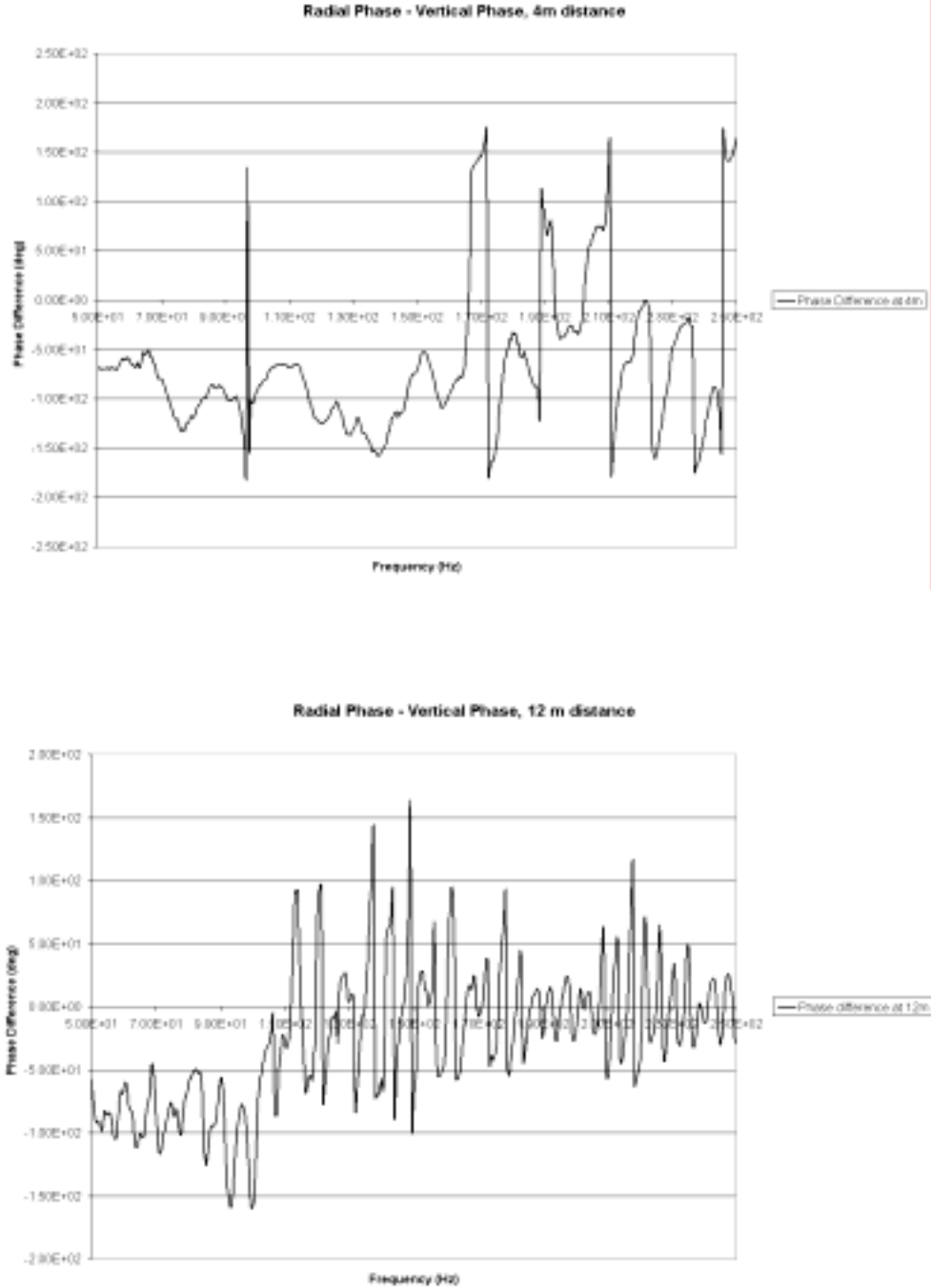


Figure 26 a) and b). Radial component of phase minus vertical component at two distances.

Frequency [Hz] is on the x-axis, and phase difference [deg] is on the y-axis. Figure 26 a) was for a geophone distance of 4m from the robot. Figure 26 b) was for a geophone 12m from the source. At low frequencies, both figures show a center on -90^0 phase difference between radial and vertical signal. A -90^0 difference indicates retrograde elliptical motion. Retrograde elliptical motion indicates the predominance of Rayleigh waves. It is interesting that the maximum frequency at which Rayleigh waves predominate decreases with increasing range. At the higher frequencies, both a) and b) show significant change, with both actually shifting their center to 0^0 . This shift is consistent with the phase of P-waves, and clearly indicates interference from P-waves. Regardless of the interference however, Figure 26 shows that Rayleigh waves were excited by the robot source. That was a very good result in terms of mine detection, as Rayleigh waves were the preferred means of detection.

The next test was to further see if only Rayleigh waves were being excited. This involved measuring the received vertical signal at various distances over a frequency scan. Figure 27 shows the data for two distances 14m (black) and 22m (gray).

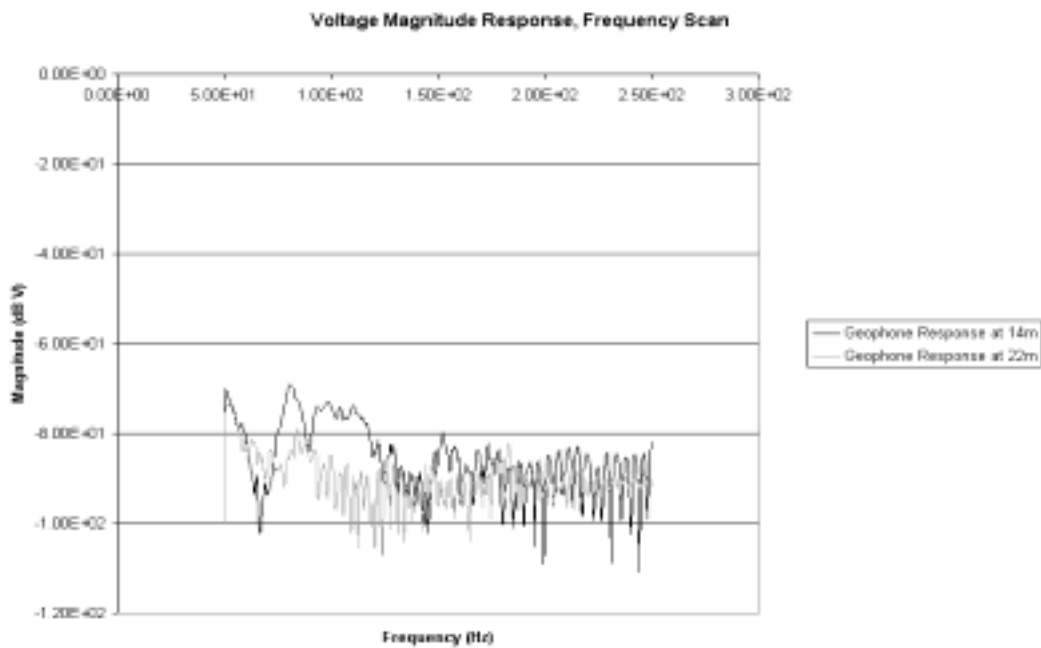


Figure 27. Vertical signal magnitude at 14m and 22m for a frequency scan.

The data that was gathered was not encouraging. At 14m there were nulls every 4 Hz, and at 22m there were nulls every 3 Hz. This led to the suspicion of destructive interference from P-Waves interfering with Rayleigh waves. Figure 28 represents what was suspected.

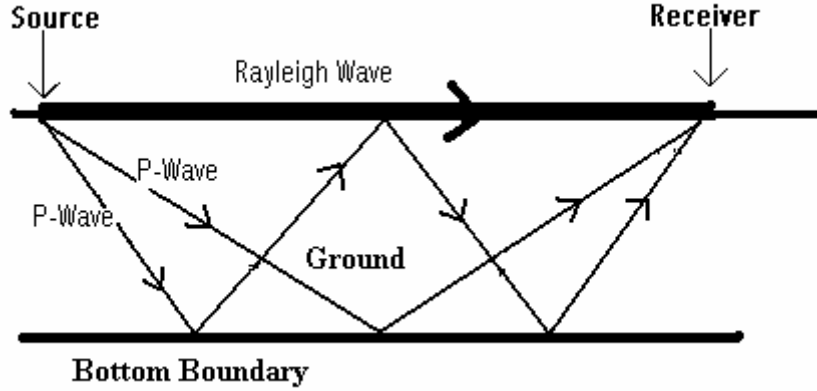


Figure 28. Bottom bounce of P-waves leading to destructive interference at the receiver.

Further confirmation of the destructive interference hypothesis was wanted. For a P-wave traveling along a single bottom reflected path, the phase of the P-wave is given by:

$$Phase = -2k_p \sqrt{h^2 + \left(\frac{l}{2}\right)^2} + \pi \quad (5.5)$$

Where k_p is the wave number of the P-wave, h is the height of the layer the wave is traveling in, and l is the horizontal distance the wave travels.

The phase difference between the Rayleigh and P-waves is then:

$$PhaseDiff = k_R l - 2k_p \sqrt{h^2 + \left(\frac{l}{2}\right)^2} + \pi \quad (5.6)$$

Where k_R is the wave number of the Rayleigh wave. Destructive interference will occur at a phase difference of $\Delta = \pi, 3\pi, 5\pi, \dots = (2m+1)\pi$; $m = 0, \pm 1, \pm 2, \dots$. After substituting in

$k = 2\pi f/c$ and some algebraic manipulation:

$$\Delta f = \frac{c_R / l}{\left[1 - \frac{c_R}{c_p} \sqrt{\left(\frac{2h}{l} \right)^2 + 1} \right]} \quad (5.7)$$

Where Δf = frequency gap between nulls, c_R = Rayleigh wave speed, and c_p = P-wave speed. Layer thickness was set at $h = 3\text{m}$, according to the advice of Tim Stanton, an associate researcher in the Oceanography Department at NPS. Calculated values for frequency gaps between nulls were 10 Hz at 14m and 6 Hz at 22m. These values did not exactly agree with estimates from looking at the data. However, they were in the same ballpark as the measured values. Also, the calculated theoretical results did show the same decrease in frequency between nulls as distance increased that the data showed. The results of the calculations were strong enough to conclude that destructive interference between P-waves and Rayleigh waves was occurring. Destructive interference could decrease Rayleigh wave amplitude, and could also lead to false alarms due to P-wave detection by sensors. Destructive interference and P-wave propagation/bottom bounce therefore would seriously hinder any attempts at target detection.

C. TARGET DETECTION

1. Detection with Oscilloscope

Despite the discouraging results from the wave classification measurements, a target search was tried just in case it actually worked. Figure 29 shows the set-up used.

(not to scale)

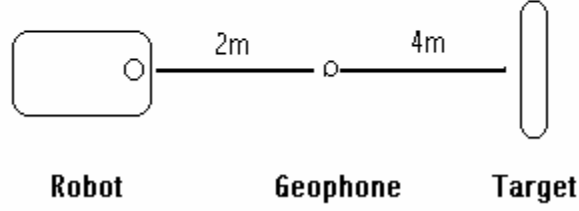


Figure 29. Set-up for target search experiment.

For the first trial, the geophone was 2m from the robot, and the target was 4m from the geophone (6m from the robot). However, many different distances between the robot and the geophone, and the geophone and the target were sampled. The target was a large air cylinder, which had a mass of 55 kg. It was buried just beneath the surface of the sand. It was hoped that the geophone would first detect the initial signal from the robot, and then detect an echo signal from the target.

Data from the target search experiment was processed using “vector polarization filtering”. Vector polarization filtering is a signal-processing technique for suppressing all but the Rayleigh waves in the received signal (Sheetz, 2000). It is based upon the fact that for a Rayleigh wave, the ground motion is elliptical and so the radial and vertical components are 90° out of phase. For a P-wave, the radial and vertical components are in phase. If $\tilde{V}_r(t)$ and $\tilde{V}_v(t)$ are the phasor representations of the radial and vertical ground motion signals, respectively, then the following complex quantity, called the “complex power”, is formed:

$$\tilde{P}_{r,v}(t) = \tilde{V}_r^*(t) \bullet \tilde{V}_v(t) . \quad (5.8)$$

Where $\tilde{P}_{r,v}(t)$ is the complex power, and \tilde{V}^* is the complex conjugate of the radial ground motion signal. The imaginary component of the complex power captures the entire Rayleigh wave signal and tends to suppress the P-wave signal. The (complex)

phasor representations of the radial and vertical ground motion signals are formed from the real-valued collected data by a Hilbert transform operation using a MATLAB M-File. The code for the program is shown in Appendix D

Figure 30 below is for a set-up with no target. Figure 31 is for a set-up with a target in place, 6m from the robot. LT Sheetz had success with target search at the 4-6m range for target search, so that is why 6m was chosen. For both tests, the drive was a single-cycle tone burst at 100 Hz, and drive voltage was 47 V peak-to-peak. Readings were recorded on the Hewlett Packard Infinium oscilloscope, with 64 averaging.

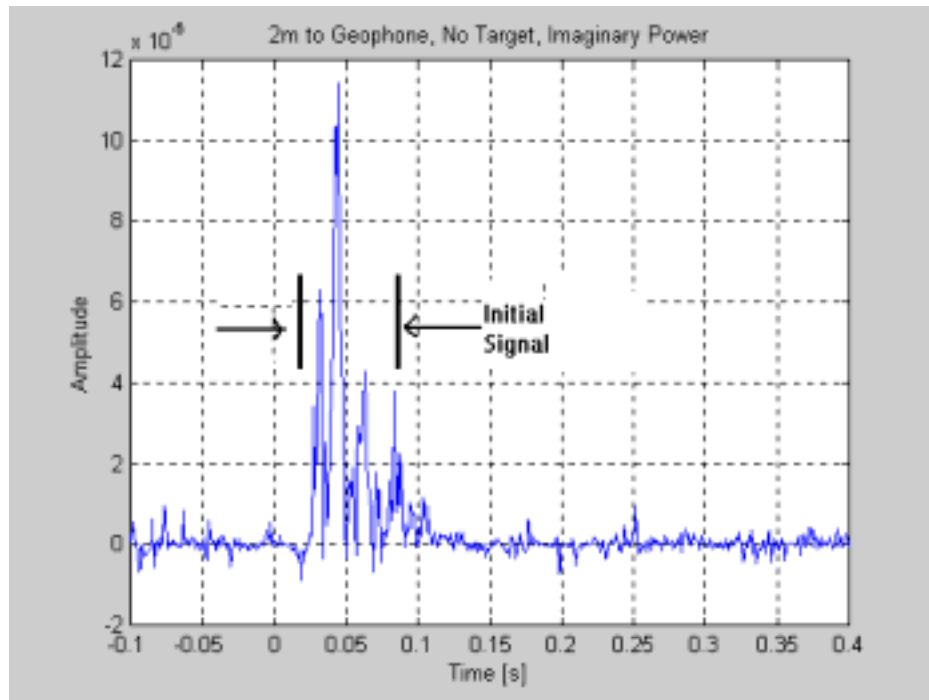


Figure 30. Imaginary part of received power at 2m from source, no target.

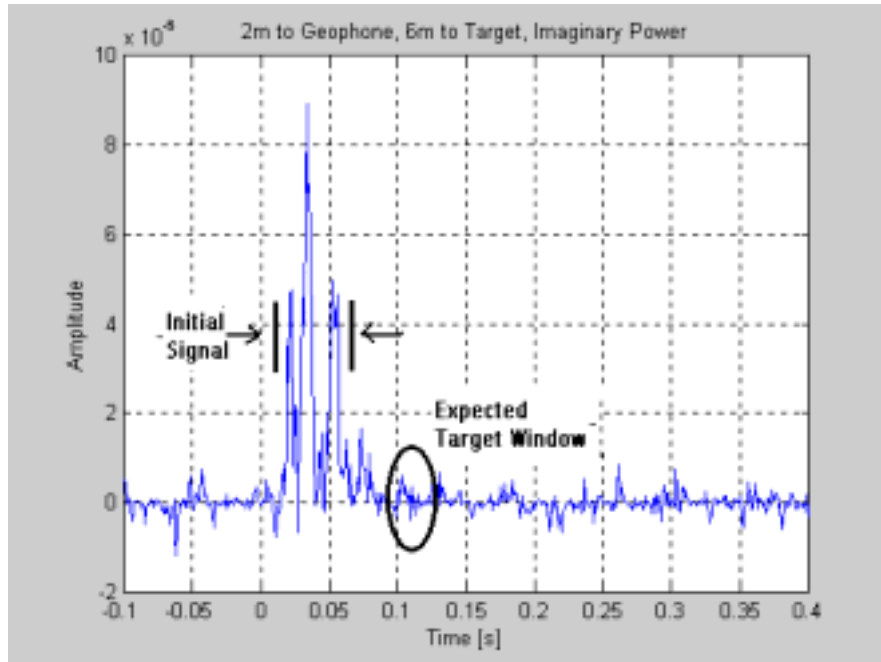


Figure 31. Imaginary part of received power at 2m from source, with a target at 6m.

For a Rayleigh wave speed of 90m/s, the initial signal was supposed to hit the geophone at time $t=0.044$ seconds. Both plots show the initial signal arriving at that expected time. On the “with target” experiment, a return signal was expected at time $t = 0.110$ s. However, the plot for the “no-target” experiment is nearly identical to the plot for the “with-target” experiment, even out at time = 0.110 seconds. This means that there was no target detection. Experiments at different distances showed the same negative results.

2. Detection with Human Ear

For curiosity sake, detection by listening was attempted. The geophone panel was used to transmit a geophone’s received signal into a stereo headphone amplifier. Headphones were then plugged into the amplifier, and the operator could actually hear the received “thump” at the geophone. Thumping could still be heard clearly at ranges of

20+ meters away from the source. However, there was a rising tone as the geophone got further away from the source. This indicated that the lower frequencies were reaching the geophone before the higher frequencies, i.e., the waves arriving at the geophone were dispersive. This dispersion is probably due to an increasing wave speed with the increasing amount of compaction, rigidity, and moisture content with depth in the sand.

Target detection by this method was then attempted. It was hoped that two separate signals could be heard through the headphones: the initial signal from the robot; and the echo signal from the target. Attempts were unsuccessful as only one thump was heard.

VI. CONCLUSIONS AND RECOMMENDATIONS

Landmines continue to be a threat to both military and civilian communities throughout the world. Current methods of detection, while better than nothing, could certainly be improved. Seismic SONAR is a promising new technology that may help save countless lives.

The goal of this thesis was to advance Seismic SONAR development by introducing a mobile source that could be easily used in practical applications. Used for a mobile source was a small tracked vehicle with dual inertial mass shakers mounted on top. The source accurately transmitted the shaker signal into the ground, and its mobility made it a practical choice for field operations. It excited Rayleigh waves, as desired, but also generated undesirable P-waves and was not directional at all. It proved incapable of finding a target.

There were three major reasons why this particular source failed for mine detection. First, it must be possible to selectively generate Rayleigh waves, while suppressing P-waves. Interference from bottom-bouncing P-waves be destructive and greatly confused signal processing. Second, more aperture is needed so that a steer-able, directional beam can be produced. This would allow the operator to know range *and* bearing for buried mines. The directionality problem may be solved by simply preferentially exciting Rayleigh waves and excluding P-waves. Third, a stronger source is needed. This could be accomplished by either a) using more shakers, or b) adding more weight to the robot. This source could be made to be effective if mounted with an array of shakers. CPT Sheetz was able to produce a highly directional beam with a strong enough signal for target detection and bearing by using a 7 element linear array of dual Aura Bass Shakers. This same concept could be applied to tracked vehicles. Figure 32 shows a possible design for mounting an array of shakers on a tracked vehicle.

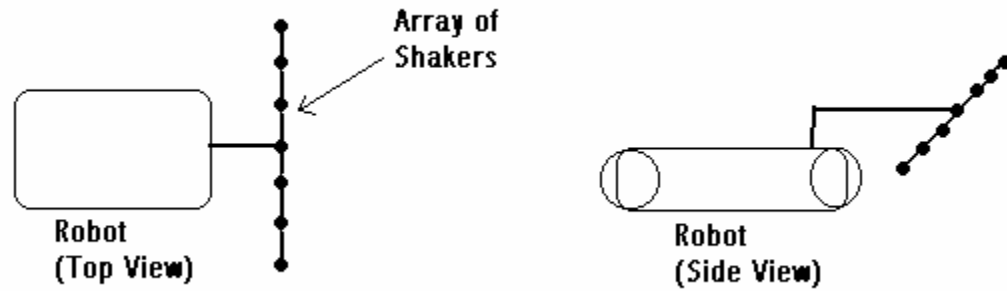


Figure 32. Proposed design for further testing.

The array could easily be lifted and lowered by means of mechanical arm, and mobility of the robot would not be compromised. Each shaker could be at a 45° angle with respect to the ground. This would preferentially excite elliptical particle motion, thus selectively producing Rayleigh waves and excluding P-waves. The concept of a tilted source selectively producing Rayleigh waves has already been shown by LT Gaghan and can work.

Seismic SONAR is still a promising means of mine detection, and it has been shown to work with a fixed, buried array of sources. Applying the concept of a large linear array and combining it with a mobile vehicle should bring seismic SONAR into the field of military use. This thesis, while not actually achieving a usable source, showed that a tracked vehicle, with improvements, is a means of mine detection with high potential.

APPENDIX A. MANUFACTURER SPECIFICATIONS FOR AURA BASS SHAKERS



Bass Shakers™ Let You Feel All the Bass without Breaking the Sound Barrier

The Bass Shaker is a transducer that generates the sensation of sound by vibration, not by moving air. The result is a big bass effect without a high pressure level that could distort sound or blow your speakers. They are also great for adding bass to vehicles with poor sound insulation, such as trucks. Mount these Bass Shakers under your front seats and you will feel the punch of the drums and the kick of the percussion, as if you were on stage or in the studio when the music was recorded! Hooks up easily to any standard audio amplifier output channel, and can be used with existing subwoofers for an extra kick. Each Bass Shaker requires only 25W RMS of power.

Model AST1B4. Item No. B-40070-492383 S/H \$9.99 ~~FREE~~

Mr. Sugg. Retail \$199.95
WAS \$179.99 \$99.99

Specifications: AST-1B-4 Bass Shaker

Frame Size: 4.75" dia. X 2.35" h

Magnet Type: Ceramic

Power Rating: Nominal 25 W

Force, Nominal: 10 lbf (44.5 N)


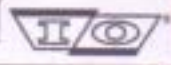
Weight: 2.5 lbs each

Resonance Frequency (fo): ... 42 Hz

Usable Frequency Range: 20-100 Hz


THIS PAGE INTENTIONALLY LEFT BLANK

APPENDIX B. MANUFACTURERS SPECIFICATIONS FOR GEOPHONES

**INPUT/OUTPUT, INC.**
SENSOR Nederland bv

SM-11 Geophone

- 30-Hz geophone with high spurious, over 500 Hz, providing wide bandwidth data suitable for up to 1-ms data sampling
- Can be operated in any orientation
- High output through the use of a special magnet and case design
- Rugged mechanical construction can withstand severe shocks
- 2-year limited warranty



The SM-11 geophone is suitable for use in extended frequency, high-resolution surveys. It has a natural frequency of 30 Hz and a spurious frequency of over 500 Hz, providing a sensor suitable for use with 1-ms sampling recording systems. The use of a special magnetic circuit makes the output of this geophone higher than normal 30-Hz geophones, ensuring adequate signal strength. The high natural frequency spring design also allows this geophone to be used in any orientation (vertical, horizontal, or inverted).

The SM-11 can be installed in the I/O Sensor PE-11 land case.

Typical application: high-resolution seismograph reflection studies.

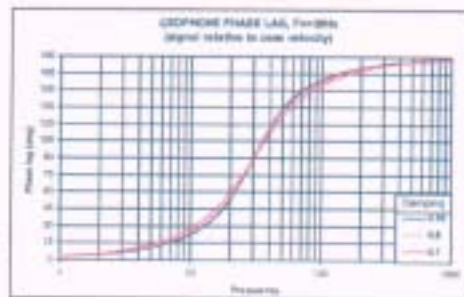
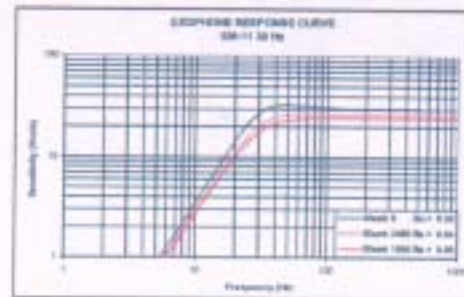
Specifications

INPUT/OUTPUT, INC.

SM-11/U-FT	
Frequency	
Natural frequency (f_n)	30 Hz
Tolerance	±5%
Maximum tilt angle for specified f_n	180°
Typical spurious frequency	>500 Hz
Distortion	
Distortion with 0.7 in/s p.p. coil-to-case velocity	<0.2%
Distortion measurement frequency	30 Hz
Maximum tilt angle for distortion specification	180°
Damping	
Open-circuit damping	0.55
Open-circuit damping tolerance	±5%
Resistance	
Standard coil resistances	360 Ω
Tolerance	±5%
Sensitivity	
Open-circuit sensitivity	30 V/m/s (0.75 V/in/s)
Tolerance	±5%
R_B/f_n	7,785 Ω/Hz
Moving mass	9.2 g (0.32 oz)
Maximum coil excursion p.p.	>1 mm (>0.04 in)
Physical Characteristics	
Diameter	26.8 mm (1.02 in)
Height	32 mm (1.26 in)
Weight	89 g (3.13 oz)
Operating temperature range	-40°C to +100°C (-40°F to +212°F)
Limited Warranty Period*	2 years

* Warranty excludes damage caused by high-voltage and physical damage to the element case.

All parameters are specified at +30°C in the horizontal position unless otherwise stated.



Ordering Information

SM-11	
SM-11/U-FT 30 Hz 360 Ω (upright)	P/N 1011010
SM-11/H-FT 30 Hz 360 Ω (horizontal)	P/N 1011030

United States – Stafford, TX
Input/Output, Inc.
Fax 281.879.3500
Phone 281.825.3338

Russia
Input/Output, Inc.
Fax 7 065.2322240
Phone 7 065.2322254

England
Input/Output, Inc.
Fax 44 1803.411403
Phone 44 1803.411400

Web Site
www.i-o.com

© 1999 Input/Output, Inc. All rights reserved. Information subject to change without notice.

121524B
01/01

APPENDIX C. MANUFACTURERS SPECIFICATIONS FOR ACCELEROMETERS

Baker Calibration Data Card
~~PC4~~ SHEAR ACCELEROMETER
 MODEL # J353803
 SERIAL # 5968

VOLTAGE SENSITIVITY: 10.05 mV/g
 FREQUENCY RANGE: 1 TO 5000 Hz
 OUTPUT BIAS LEVEL: 8.4 V
 Date: 2-21-94 By: M.R.

For further information please refer to
Calibration Certificate.



3425 Walden Ave • Depew, NY-14043
 (716) 684-0001

Baker Calibration Data Card
~~PC4~~ SHEAR ACCELEROMETER
 MODEL # J353803
 SERIAL # 9319

VOLTAGE SENSITIVITY: 10.24 mV/g
 FREQUENCY RANGE: 1 TO 7000 Hz
 OUTPUT BIAS LEVEL: 8.4 V
 Date: 1-25-94 By: G.R.

For further information please refer to
Calibration Certificate.



3425 Walden Ave • Depew, NY-14043
 (716) 684-0001

THIS PAGE INTENTIONALLY LEFT BLANK

APPENDIX D. MATLAB CODE FOR “HILBRT.M”

```
% Name: Hilbrt.m
% Author: LT Mike Fitzpatrick
% Updated: 05/30/03 by ENS Doug MacLean
% Description: This subroutine conducts a Hilbert analysis of the
% geophone signals for vector polarization filtering.
% This is a versatile program meant to output the
% imaginary and real parts of a received signal. There
% are various user-selectable features

%%%Input Parameters%%%
Range=1; %Turns-on plotting with range axis
wavespd=296; %Wavespeed [ft/s]

%%%Date, Directory, & File%%%
clc,disp('***Hilbert Analysis Subroutine***'); disp(' ');
if exist('date')~=1, dir *.* ,
    date=input('Enter the date --> ','s');
end

clc,disp('***Hilbert Analysis Subroutine***'), dir *.*
directory=input('Enter the directory --> ','s');
cd (directory);
clc,disp('***Hilbert Analysis Subroutine***'), dir *.mat;
file=input('Enter filename --> ','s'); disp(' ');
data=xlsread(file);

transform=hilbert(data);
```

```

Pwr(:,1)=conj(transform(:,1)).*transform(:,2);

    directory=input('Enter the directory for time vector -->
','s');
    cd (directory);
    clc,disp('***Hilbert Analysis Subroutine***'), dir *.mat;
    timeFile=input('Enter filename for time vector--> ','s');
disp(' ');
    t=xlsread(timeFile);

    %%%Plotting%%%
    figure (1)
        plot(t,real(Pwr))
        title('Real Power --> ')
        ylabel('Amplitude'),grid
        %%%%%%%%%%%%%
    figure (2)
        plot(t,imag(Pwr))
        title('Imaginary Power')
        xlabel('Time [s]')
        ylabel('Amplitude'),grid

```

LIST OF REFERENCES

1. Sheetz, Kraig E., *Advancements in Buried Mine Detection Using Seismic SONAR*, Master's Thesis, Naval Postgraduate School, December 2002
2. Gaghan, Frederick E., *Discrete Mode Source Development and Testing For New Seismo-Acoustic SONAR*, Master's Thesis, Naval Postgraduate School, March 1998
3. Vietnam Veterans of America Foundation (VVAF), "1999 VVAF Annual Report", [vvaf.policy.net/about/annualreport.pdf], December 1999. Accessed 19 May, 2003
4. Rachel Stohl, "Lessons Learned – Using Landmines in a War with Iraq", [<http://www.cdi.org/terrorism/gulf-landmines-pr.cfm>], November, 2002. Accessed 19 May, 2003
5. Zamora, George, "Detecting Land Mines." [<http://www.nmt.edu/mainpage/news/landmine.html>]. September, 1997. Accessed 20 May, 2003
6. Dolphin, Lambert, "Ground Penetrating Radar Usage and Limitations", [<http://www.ldolphin.org/GPRLimits.html>], November 1997. Accessed 20 May, 2003
7. Geophysics Department, St. Andrew's University, "Introduction to Geophysics", [http://www.standrews.ac.uk/~www_sgg/personal/crblink/web/2yrintrogp/g2p.html]. Accessed 24 May, 2003
8. Brown G.C. & Musset A.E., *The Inaccessible Earth*, George Allen and Unwin Ltd., 1981
9. Fitzpatrick, Sean M., *Source Development for a Seismo-Acoustic SONAR*, Master's Thesis, Naval Postgraduate School, December 1998
10. Richart, F.E., Hall, J.R., Woods, R.D., *Vibration of Soils and Foundations*, Prentice Hall, Inc., 1970

11. Seismology Lab, California Institute of Technology, [http://www.gps.caltech.edu/~polet/body_waves.html]. Accessed 29 May, 2003.
12. Chiarella, Chris, “The Guitammer Company ButtKicker Shaker”, *Home Theater* magazine, May 2001
13. Kinsler, L.E, Frey, R.F., Coppens, A.B., Sanders, J.V., *Fundamentals of Acoustics*, Fourth Edition, John Wiley & Sons, Inc., 2000
14. McClelland, Scott C., *A Rolling Line Source for a Seismic SONAR*, Master’s Thesis, Naval Postgraduate School, June 2002
15. Hall, Patrick W., *Detection and Target Strength Measurements of Buried Objects, Using a Seismo-Acoustic SONAR*, Master’s Thesis, Naval Postgraduate School, December 1998
16. Stewart, William F., *Buried Object Detection Using Surface Waves*, Master’s Thesis, Naval Postgraduate School, September 1995

INITIAL DISTRIBUTION LIST

1. Dudley Knox Library
Naval Postgraduate School
Monterey, CA
2. Professor Steven R. Baker, Code PH/Ba
Department of Physics
Naval Postgraduate School
Monterey, CA
3. ENS Douglas J. MacLean
Vestal, NY
4. LT Steven Rumph
042 Spanagel Hall
Naval Postgraduate School
Monterey, CA
5. Professor Thomas G. Muir
University of Mississippi
University, MS
6. Dr. Douglas Todoroff
Office of Naval Research, Code 322W
Arlington, VA
7. Dr. James Luscombe, Code PH
Department of Physics
Naval Postgraduate School

Monterey, CA

8. Defense Technical Information Center

Ft. Belvoir, VA